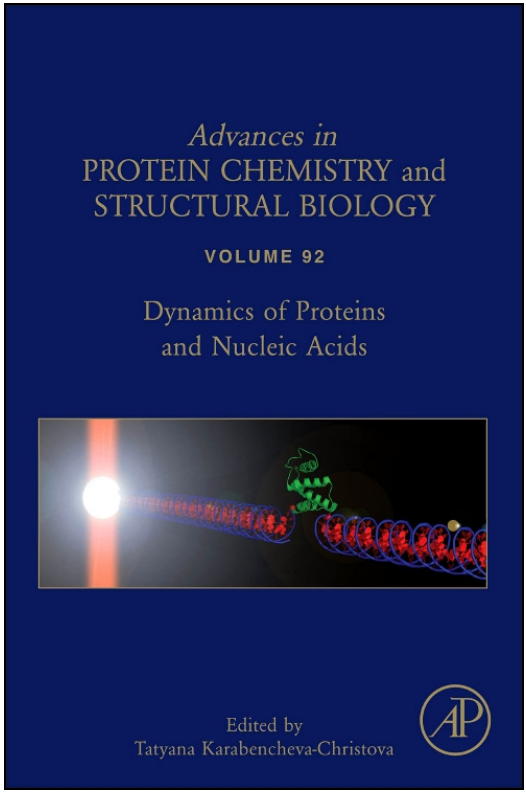

From: Pétur O. Heidarsson, Mohsin M. Naqvi, Punam Sonar, Immanuel Valpapuram, Ciro Cecconi, Conformational Dynamics of Single Protein Molecules Studied by Direct Mechanical Manipulation. In Tatyana Karabencheva-Christova, editors: *Advances in Protein Chemistry and Structural Biology,* Vol. 92,
Burlington: Academic Press, 2013, pp. 93-133.
ISBN: 978-0-12-411636-8

CHAPTER THREE

Conformational Dynamics of Single Protein Molecules Studied by Direct Mechanical Manipulation

Pétur O. Heidarsson[*], Mohsin M. Naqvi[†], Punam Sonar[†], Immanuel Valpapuram[†], Ciro Cecconi[‡,1]

[*]Structural Biology and NMR Laboratory, Department of Biology, University of Copenhagen, Copenhagen N, Denmark
[†]Department of Physics, University of Modena and Reggio Emilia, Modena, Italy
[‡]CNR Institute of Nanoscience S3, University of Modena and Reggio Emilia, Modena, Italy
[1]Corresponding author: e-mail address: ciro.cecconi@gmail.com

Contents

Abstract

Advances in single-molecule manipulation techniques have recently enabled researchers to study a growing array of biological processes in unprecedented detail. Individual molecules can now be manipulated with subnanometer precision along a simple and well-defined reaction coordinate, the molecular end-to-end distance, and their

Advances in Protein Chemistry and Structural Biology, Volume 92
ISSN 1876-1623
http://dx.doi.org/10.1016/B978-0-12-411636-8.00003-1

conformational changes can be monitored in real time with ever-improving time resolution. The behavior of biomolecules under tension continues to unravel at an accelerated pace and often in combination with computational studies that reveal the atomistic details of the process under investigation. In this chapter, we explain the basic principles of force spectroscopy techniques, with a focus on optical tweezers, and describe some of the theoretical models used to analyze and interpret single-molecule manipulation data. We then highlight some recent and exciting results that have emerged from this research field on protein folding and protein–ligand interactions.

ABBREVIATIONS

AFM atomic force microscopy
CaM calmodulin
CFT Crooks' fluctuation theorem
HMM hidden Markov model
MD molecular dynamics
NMR nuclear magnetic resonance
WLC worm-like chain

1. INTRODUCTION

Sophisticated bulk methods have been developed to characterize the conformational changes of proteins as they carry out their biological functions. Traditional techniques such as circular dichroism, nuclear magnetic resonance (NMR) spectroscopy, and hydrogen/deuterium exchange mass spectrometry (Greenfield, 2007; Kern, Eisenmesser, & Wolf-Watz, 2005; Maity, Maity, Krishna, Mayne, & Englander, 2005) have been extensively used to study the structure and dynamics of proteins, both free in solution or bound to their molecular partners. These bulk studies have been very informative but limited to the description of the overall properties of a large population of proteins. This is because the output from these measurements is the ensemble average generated from a large, and often dephased, population of molecules, in which the time-dependent dynamics of the individual molecules, as well as rare but potentially important molecular events, are hidden. These technical limitations, which have restrained our ability to decipher the intricacies of many molecular processes, have recently been overcome with the advent of single-molecule methods. These novel experimental approaches enable us to follow the real-time trajectories of single molecules and describe the inherent heterogeneity of biological processes that are stochastic in nature.

Single-molecule detection methods are mainly based on fluorescence intensity or energy transfer efficiency between fluorophores, using either freely diffusing or surface-tethered molecules. Several excellent papers that review fluorescence-based single-molecule techniques have been published elsewhere (Borgia, Williams, & Clarke, 2008; Deniz, Mukhopadhyay, & Lemke, 2008; Joo, Balci, Ishitsuka, Buranachai, & Ha, 2008; Schuler & Eaton, 2008; Tinoco & Gonzalez, 2011). In this review, we focus exclusively on mechanical manipulation methods, specifically optical tweezers and atomic force microscopy (AFM) and illustrate the main experimental strategies used in these techniques. We then go on to describe some theoretical models employed in this field, before highlighting some pivotal single-molecule studies aimed at solving exciting biological problems. Due to space limitations and the fast expansion of the field, it is impossible for us to review all recently published studies and we refer the reader to other reviews for a more comprehensive overview of the field (Borgia et al., 2008; Bustamante, 2008; Deniz et al., 2008; Moffitt, Chemla, Smith, & Bustamante, 2008).

2. MECHANICAL MANIPULATION OF SINGLE PROTEIN MOLECULES

Just as chemicals and heat can be used to perturb the system under study, so can force be used for the same purpose. Force and the end-to-end distance of a protein molecule constitute the main variables during a mechanical manipulation experiment. Many methods have been developed to directly manipulate biomolecules. In this chapter, we briefly discuss the two most popular experimental methods, optical tweezers and AFM.

2.1. Optical tweezers

Ever since the pioneering work of Arthur Ashkin in the 1980s (Ashkin, Dziedzic, Bjorkholm, & Chu, 1986), optical tweezers have continued to evolve and improve to tackle ever more complex systems. An optical trap can be formed by focusing a collimated beam of light through a microscope objective with a high numerical aperture. In this way, small objects of high refractive index can be optically trapped and manipulated. For a detailed description of the principles behind optical trapping, which is beyond the scope of this chapter, we refer the reader to previous publications (Ashkin et al., 1986; Moffitt et al., 2008; Smith, Cui, & Bustamante, 2003). There are three main geometries that are nowadays used in the optical tweezers setups (Fig. 3.1).

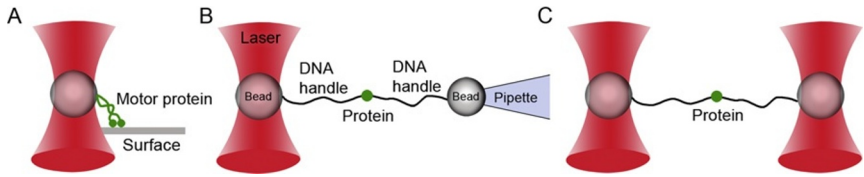

Figure 3.1 Optical tweezers experimental geometries. (A) A single-beam optical tweezers setup where the molecule of interest is tethered between an optically trapped bead and a surface. The movements of the protein along the surface are revealed by the motions of the bead in the trap. (B) A single-beam optical tweezers experimental setup where the protein is attached to two polystyrene beads through two double-stranded DNA handles. One bead is held in the optical trap while the other is held at the end of a micropipette by suction. The micropipette can be mechanically moved relative to the trap, to induce the unfolding or refolding of a protein molecule. (C) A double-beam setup where the protein molecule is tethered through DNA handles between two optically trapped beads. See text for details.

In all cases, the molecule under study is tethered between an optically trapped bead and: (i) a substrate, (ii) a second bead held at the end of micropipette by suction, or (iii) another bead held in a second optical trap. In all cases, the force applied to the molecule is modulated by varying the distance between the two tethering points. Different approaches can be taken to manipulate a molecule. In what follows, we briefly describe the experimental strategy used in: (i) constant-velocity (also force-ramp), (ii) constant-force (also force-clamp), (iii) passive-mode, and (iv) force-jump experiments. In constant-velocity experiments, the force is increased and relaxed at constant speed (nm/s), to obtain force versus extension cycles as shown in Fig. 3.2A. During stretching, the force is raised until the molecule is observed to unfold. This event is marked by a sudden increase in the extension of the molecule, as it goes from its compact native state (N) to a more extended unfolded state (U). During relaxation, the molecule is typically observed to refold around at ~5–10 pN, through a sharp transition that restores the original extension of the molecule. The changes in contour length of the protein associated with the unfolding and refolding events can be estimated by fitting the force–extension traces with the worm-like chain (WLC) model (Bustamante, Marko, Siggia, & Smith, 1994; Cecconi, Shank, Bustamante, & Marqusee, 2005; Liphardt, Onoa, Smith, Tinoco, & Bustamante, 2001). Constant-velocity experiments can provide information on both kinetics and thermodynamics of a protein folding reaction. Kinetic parameters, such as rate constants and position of the transition

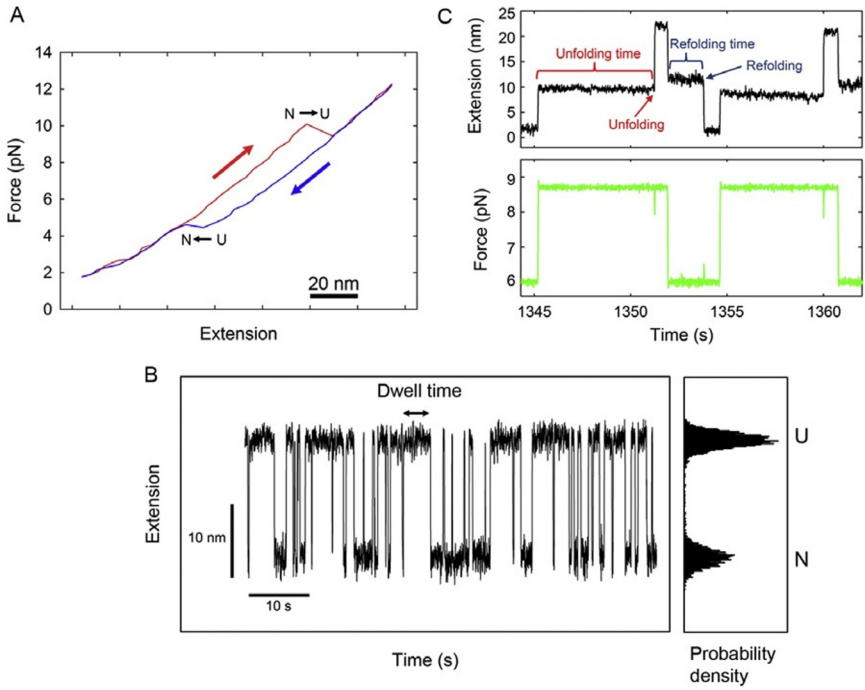

Figure 3.2 Basic mechanical manipulation experiments using optical tweezers. (A) Constant-velocity experiment showing a two-state unfolding/refolding event. The arrows indicate the pulling direction. (B) Constant-force experiment showing a molecule fluctuating between an unfolded (U) and folded (N) state. The dwell times of the unfolded and folded states contain both thermodynamic and kinetic information. (C) Force-jump experiment. The force is rapidly jumped between two different set values, to increase the probability of observing unfolding/refolding events, see text for details. *Adapted from Heidarsson et al. (2012) with permission.*

state along the reaction coordinate, can, for example, be estimated by analyzing force distributions. Thermodynamics information (e.g., unfolding free energy) can instead be recovered by analyzing irreversible work distributions (see below for details).

In constant-force experiments, the force applied to the molecule is kept constant through a feedback mechanism, while changes in the extension of the molecule are monitored over time (Fig. 3.2B). In these measurements, rate coefficients can be obtained directly from the lifetimes of the folded and unfolded states, and free energies can be calculated from the ratio of the kinetics coefficients. As the molecule unfolds or refolds, the force is kept constant by reducing or increasing the distance between the tethering

surfaces, respectively. These movements, which are controlled by the feedback mechanism, can, however, take place only at a certain rate and, because of this constant force, measurements can sometimes provide misleading results. This is the case, for example, when the response rate of the feedback mechanism is slower than the rate at which the molecule can fluctuate. In these cases, in fact, short-lived transitions are missed, leading to average dwell times biased toward larger values (Elms, Chodera, Bustamante, & Marqusee, 2012b). This potential instrumental artifact can be avoided, or at least reduced, by studying molecular fluctuations through passive-mode measurements. In this case, no feedback is employed. Instead, the distance between the tethering surface and the optical trap is kept constant, while force is allowed to increase or decrease as the molecule unfolds or refolds, respectively. In these experiments, the response time of the system is dictated by the corner frequency of the trapped bead, which is typically much higher than the response frequency of a feedback mechanism. Consequently, passive-mode measurements are better suited to study rapid conformational transitions. On the other hand, as no feedback mechanism is used, reliable passive-mode measurements require high mechanical and optical stability of the instrument itself.

Constant-force or passive-mode measurements can be effectively used to study molecular fluctuations at equilibrium only when, in a certain range of forces, the rate of both the forward and reverse reactions is high enough to allow the acquisition of a large number of events in a relatively short amount of time. This, however, is not always the case, as for some molecules unfolding and refolding occurs at quite different forces. In these instances, at any given force, either the unfolding or refolding rate is so low that the acquisition of a significant number of events would require very long recordings. To overcome this problem, force-jump experiments can be performed. In a force-jump experiment, the force is increased (jumped) or decreased (dropped) quickly to a preset force value and kept constant with a feedback mechanism until an unfolding or refolding event is observed (Fig. 3.2C). These experiments allow the direct measurement of rate constants in force ranges where the probability of observing either an unfolding or refolding event is high (Li, Collin, Smith, Bustamante, & Tinoco, 2006).

2.1.1 Alternative, novel, and hybrid optical tweezers instruments

Single-molecule manipulation instruments are advancing at a rapid pace. Considerable effort has been spent on designing optical tweezers that measure other single-molecule parameters such as rotation or torque in

combination with force and extension (Neuman & Nagy, 2008). The ability to measure torque has significant importance because it addresses many aspects of cell and protein biology such as transcription, replication, recombination, and protein folding (De Vlaminck et al., 2010; Koster, Crut, Shuman, Bjornsti, & Dekker, 2010). The measurement of torque can be achieved with magnetic tweezers, a popular instrument because it is simple and cheap (De Vlaminck & Dekker, 2012). Spatial and temporal resolution of magnetic tweezers may in the near future advance to subnanometer precision, possibly with newly emerging camera technology that enhances the rate of data acquisition (De Vlaminck & Dekker, 2012).

The integration of dual beam optical tweezers with magnetic tweezers allows manipulation of a single molecule with nanometer precision. This hybrid instrument has been used to investigate a wide range of complex systems such as higher order chromatin interaction, DNA–DNA interaction mediated by proteins, measurement of intermolecular friction and localization, and binding strength analysis of DNA bound proteins (Noom, van den Broek, van Mameren, & Wuite, 2007). The combination of magnetic or optical tweezers and fluorescence microscopy is a powerful tool for DNA manipulation and has been used to study DNA supercoiling, the dynamics of diffusion, hopping of plectonemics in DNA, and the torque and twist DNA-breathing dynamics (De Vlaminck, Henighan, van Loenhout, Burnham, & Dekker, 2012; Sirinakis, Ren, Gao, Xi, & Zhang, 2012).

A recently designed Quad-trap optical tweezers instrument was used to study the condensation of bacterial chromosome DNA (Dame, Noom, & Wuite, 2006). The instrument was able to independently trap four polystyrene beads at the same time, allowing the simultaneous mechanical manipulation of two independent DNA molecules. With this method, the authors were able to detect the complex and dynamic interactions of DNA and histone-like nucleoid structuring protein (H-NS), which is involved in mediating DNA–DNA contact. This remarkable technical feature helped explain the mechanism and role of H-NS in chromosomal DNA condensation.

2.1.2 Sample preparation

A major issue in optical tweezers experiments is to find an efficient method to manipulate the molecule of interest. Biomolecules such as proteins and RNAs are typically too small to be directly manipulated with micrometer-sized optical tweezer beads, as the tethering surfaces would come so close to each other that they would interact. To avoid these

unspecific and unwanted interactions, a method has been developed that relies on the use of two DNA molecular handles (Fig. 3.1B and C) (Cecconi, Shank, Dahlquist, Marqusee, & Bustamante, 2008). One end of each handle (~500–1000 bp DNA molecule) is attached covalently to the side chain of a cysteine residue. The other end is attached to a polystyrene bead through either biotin–streptavidin interactions or digoxigenin/antibody interactions. The handles act as spacers between the protein and the beads to avoid unwanted interactions between the tethering surfaces that would compromise the experiment. This optical tweezers manipulation method was employed for the first time in 2005 (Cecconi et al., 2005), and it is now used by a growing number of laboratories around the world (Gao, Sirinakis, & Zhang, 2011; Gebhardt, Bornschlogl, & Rief, 2010; Stigler & Rief, 2012; Xi, Gao, Sirinakis, Guo, & Zhang, 2012; Yu, Liu, et al., 2012). For details on how the DNA–protein coupling reaction is performed, we refer the reader to Cecconi, Shank, Marqusee, and Bustamante (2011).

2.2. Atomic force microscopy

AFM was initially developed for high-resolution imaging of surface contours of microscopic samples (Binnig, Quate, & Gerber, 1986) and it still primarily serves this function. Later, AFM also evolved into a versatile technique to manipulate single molecules and characterize their mechanical properties, in a mode of operation called "force spectroscopy" or "force measuring." AFM force spectroscopy has been used to study a number of biological systems, including binding of antibodies to their antigens (Raab et al., 1999), ligand to receptors (Florin, Moy, & Gaub, 1994), binding forces of complementary DNA strands (Lee, Chrisey, & Colton, 1994), conformational changes in biological polymers (Rief, Oesterhelt, Heymann, & Gaub, 1997), and to study the mechanical properties of a large variety of protein molecules (Bornschlogl & Rief, 2011; Garcia-Manyes, Dougan, Badilla, Brujic, & Fernandez, 2009; Ng, Randles, & Clarke, 2007; Rounsevell, Forman, & Clarke, 2004).

When AFM is used to study protein folding, the molecule of interest, typically a polyprotein made of a linear array of a globular domain, is tethered between a flat surface, usually made of gold, and a silicon nitrite AFM tip (Fig. 3.3A). One end of the polyprotein interacts with the gold surface through thiol groups of terminal cysteine residues, while the other end adheres to the tip unspecifically. The polyprotein is then stretched and

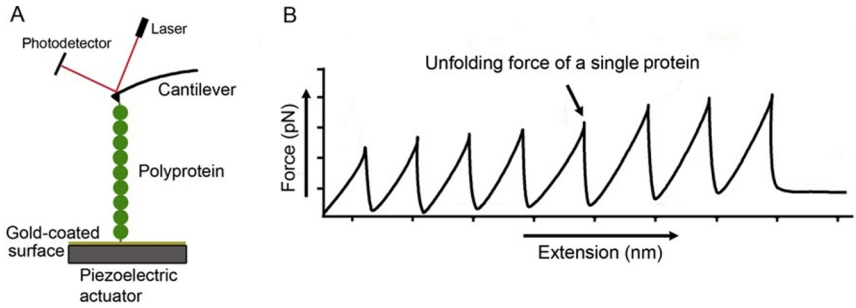

Figure 3.3 An AFM experiment. (A) In a typical AFM experiment, polyprotein constructs are picked up and unfolded by the cantilever tip. The position of the tip is determined by a photodetector from the deflection of a laser beam. (B) The sequential unfolding of single proteins within the polyprotein construct results in a characteristic sawtooth pattern in the force versus extension trace.

relaxed by modulating the distance between the tethering surfaces, while the force applied on the molecule is determined by measuring the deflection of the cantilever. As the tip is pulled away from the surface, the tension along the polymer increases until one globular domain stochastically unfolds. Upon unfolding, the contour length of the polymer suddenly increases, generating a sharp drop of the force on the cantilever. As the stretching of the polymer continues, all the other domains subsequently unfold, generating a series of sudden force drops that give rise to a peculiar sawtooth-like pattern in the force–extension curve, where each peak corresponds to the unfolding of one domain (Fig. 3.3B). The rising phase of each peak reflects the elastic properties of the stretched polymer, while the distance between peaks is proportional to the number of amino acids constituting the protein domain. As in optical tweezers experiments molecular handles are necessary to keep the two polystyrene beads away from each other, in AFM studies the need for polyproteins comes from the necessity of keeping a certain distance between the tip and the substrate. At short distances, in fact, tip–surface interactions could become the dominant features of a force trace. Different methods have been devised to generate a linear array of a globular domain, as described in Carrion-Vazquez et al. (1999), Cecconi et al. (2008), Dietz, Bertz, et al. (2006), Steward, Toca-Herrera, and Clarke (2002), and Yang et al. (2000). AFM force spectroscopy experiments on polyproteins can be performed at different pH and ionic strengths, as well as in the presence of other molecules to study the effect of binding partners on the energetics of the protein (Junker & Rief, 2009; Junker, Ziegler, & Rief, 2009).

AFM and optical tweezers are complementary techniques for the study of the mechanical properties of biomolecules. An AFM cantilever has a higher root-mean square force noise (~15 pN) than an optically trapped bead (~0.1 pN). As a consequence, optical tweezers is the technique of choice to study processes that take place at low forces, such as the refolding of a protein, that typically occur in a 5–10 pN force range. In addition, the shallower harmonic potential of an optical trap, compared to an AFM cantilever, makes laser tweezers a better technique to observe a molecule hopping between different molecular states. In fact, the steeper the harmonic potential, the larger is the kinetic barrier that the system molecule-force transducer must overcome to hop between a folded and unfolded state of the molecule. On the other hand, optical tweezers are usually unable to measure forces that are larger than 100 pN, while AFM can measure forces even in the nanoNewton range. It follows that AFM is the technique of choice to measure the rupture force of single covalent bonds (~2 nN) (Grandbois, Beyer, Rief, Clausen-Schaumann, & Gaub, 1999), the force at which polysaccharides switch to different conformations (~270 pN) (Marszalek, Oberhauser, Pang, & Fernandez, 1998), or to characterize the mechanical properties of proteins that unfold at high forces (Dietz, Berkemeier, Bertz, & Rief, 2006).

3. THEORETICAL MODELS OF SINGLE-MOLECULE FORCE SPECTROSCOPY

The mechanical manipulation of single molecules using optical tweezers and AFM can yield valuable information about the free-energy surface of a single-molecule reaction. In this section, using basic thermodynamic and kinetic principles, we explain the effect of mechanical force on the energy landscape of a molecule. Then, we discuss some theoretical models used to analyze and interpret single-molecule manipulation results.

3.1. Effect of force on the thermodynamics of a single-molecule reaction

The effect of force on a two-state reaction in which A is converted into B is depicted in Fig. 3.4. Along the mechanical reaction coordinate, which is an extension of the molecule, states A and B occupy free-energy minima separated by a distance Δx.

The free-energy difference between A and B at zero force is

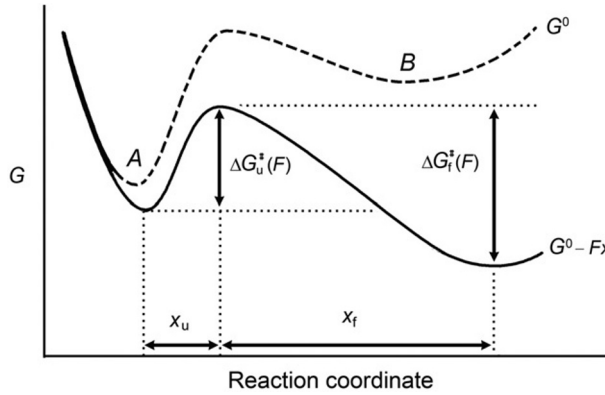

Figure 3.4 Energy landscape for a two-state unfolding reaction. The dotted-line curve is the free-energy surface at force = 0 and the solid-line curve at force = *F*. The force *F* tilts the energy landscape by a factor *Fx*, where *x* is the extension of the molecule.

$$\Delta G(F=0) = \Delta G^{\circ} + k_{\mathrm{B}} T \ln\left(\frac{[B]}{[A]}\right) \tag{3.1}$$

where ΔG° is the standard state free energy, $k_{\mathrm{B}}T$ is the thermal energy, and $[A]$ and $[B]$ give the probabilities of populating states A and B in single-molecule experiments. To a first approximation, when a force F is applied to a molecule, each point of its energy landscape is lowered by an amount equal to $F\Delta x$, where Δx is the distance between the point of interest and the native state. As a consequence, an applied force tilts the free-energy surface along the mechanical reaction coordinate (Bustamante, Chemla, Forde, & Izhaky, 2004), such that

$$\Delta G(F) = \Delta G^{\circ} - F(\Delta x) + k_{\mathrm{B}} T \ln\left(\frac{[B]}{[A]}\right) \tag{3.2}$$

At equilibrium, $\Delta G = 0$ and

$$\Delta G^{\circ} = -k_{\mathrm{B}} T \ln K_{\mathrm{eq}}(F) + F\Delta x \tag{3.3}$$

Equation (3.3) holds true only if the position of A and B along the reaction coordinate are unaffected by force. For most reactions, however, this is not true. Let us consider, for example, the case of a protein that under tension transits from its native state to its unfolded state. In this case, the extension of the native state, and thus its position along the reaction coordinate, can to a good approximation be considered unchanged, but the extension of the unfolded state instead will significantly increase. This increment in the

average end-to-end distance of the unfolded state corresponds to a change in the free energy of the system, as

$$\Delta G^{\circ} = -k_B T \ln K_{eq}(F) + F\Delta x - \Delta G_{stretch}(F) \tag{3.4}$$

where $\Delta G_{stretch}(F)$ is the free-energy change due to stretching of the unfolded state at force F. When a molecule is manipulated at close to equilibrium conditions, it unfolds and refolds through transitions that take place around a force ($F_{1/2}$) at which the molecule has equal probability of being either in its folded or unfolded state. At $F_{1/2}$, $K_{eq}=1$ and

$$\Delta G^{\circ} = F_{1/2}\Delta x - \Delta G_{stretch}\left(F_{1/2}\right) \tag{3.5}$$

Under these experimental conditions, $F_{1/2}\Delta x$ can be calculated as the area under the unfolding/refolding rips observed in force versus extension curves. This free energy can then be compared with that measured in bulk measurements after subtraction of $\Delta G_{stretch}(F_{1/2})$, which can to a good approximation be calculated as the area under the WLC force–extension curve integrated from zero to the extension of the unfolded molecule at $F_{1/2}$ (Cecconi et al., 2005; Liphardt et al., 2001).

3.2. Effect of force on the kinetics of a single-molecule reaction

As we know from transition state theory, the rates of unfolding (k_u^0) and refolding (k_f^0) of a molecule at zero force are

$$k_u^0 = A\exp\left(\frac{-\Delta G_u}{k_B T}\right) \tag{3.6}$$

$$k_f^0 = A\exp\left(\frac{-\Delta G_f}{k_B T}\right) \tag{3.7}$$

where A is the natural frequency of oscillation, ΔG_u and ΔG_f are the activation energies for unfolding and refolding, respectively. In the presence of force, the unfolding (ΔG_u) and refolding (ΔG_f) activation energies will be lowered by an amount equal to $F\cdot\Delta x_u$ and $F\cdot\Delta x_f$, respectively, where Δx_u and Δx_f are the distances to the transition state from the unfolded and folded states (Bell, 1978). It follows that the unfolding and refolding rates at force F are given by:

$$k_u(F) = k_u^0\exp\left(\frac{F\Delta x_u}{k_B T}\right) \tag{3.8}$$

$$k_f(F) = k_f^0 \exp\left(\frac{-F\Delta x_f}{k_B T}\right) \tag{3.9}$$

From the ratio of $k_u(F)$ and $k_f(F)$, the equilibrium constant can be calculated as:

$$K_{eq}(F) = K_{eq}^0 \exp\left(\frac{F\Delta x}{k_B T}\right) \tag{3.10}$$

where K_{eq}^0 is the equilibrium constant at zero force and $\Delta x = \Delta x_u + \Delta x_f$.

It is worth pointing out that in the above kinetics models, the position of the transition state along the reaction coordinate is considered to be independent from the applied force. This approximation is usually correct when we consider a very narrow range of forces. For more general cases, however, force-induced shifts in the position of the transition state must be accounted for. To this end, several improved models have been proposed and applied to different systems, as for example in Dudko, Graham, and Best (2011), Manosas, Collin, and Ritort (2006), and Schlierf, Berkemeier, and Rief (2007).

3.3. Extracting kinetic parameters from force distributions

In constant-velocity optical tweezers experiments (Fig. 3.2A), above 3–4 pN, the rate at which the force is applied on the molecule, loading rate r (dF/dt in units of pN/s), typically becomes constant (Cecconi et al., 2005; Liphardt et al., 2001). This allows us to analyze experimental data with analytical models, as explained below.

For a first-order reaction with negligible refolding rate, the time dependence of the probability that the molecule has not unfolded is (Tinoco & Bustamante, 2002):

$$\frac{dP_f(t)}{dt} = -k_u(t)P_f(t) \tag{3.11}$$

If force varies linearly with time t as $F = r\,t$, where r is the loading rate, then variable t can be changed to F in the above equation as

$$\frac{dP_f(F)}{dF} = -\frac{k_u(F)}{r}P_f(F) \tag{3.12}$$

Integrating the above equation from 0 to F and using Eq. (3.8), we get

$$\ln\{P_f(F)\} = \frac{k_u^0 k_B T}{r x_u}\left(1 - \exp\left(\frac{F x_u}{k_B T}\right)\right) \tag{3.13}$$

From Eq. (3.13), the probability of unfolding as a function of force ($P_u(F)$) can be derived as

$$P_u(F) = 1 - P_f(F) = 1 - \exp\left(-\frac{k_u^0 k_B T}{(r x_u)(\exp(F x_u / k_B T) - 1)}\right) \tag{3.14}$$

By differentiating $P_u(F)$, which is a sigmoidal function of force, we can calculate the probability density as

$$\frac{dP_u}{dF} = \frac{k_u^0}{r}\exp\left(\frac{F x_u}{k_B T}\right) * \exp\left(-\frac{k_u^0 k_B T}{(r x_u)(\exp(F x_u / k_B T) - 1)}\right) \tag{3.15}$$

Following similar steps, the probability density function for the refolding force can be calculated as

$$\frac{dP_f}{dF} = \frac{k_f^0}{r}\exp(-F x_f / k_B T) * \frac{\exp\left(-\frac{k_f^0 k_B T}{r x_f}\left(\exp\left(-\frac{F x_f}{k_B T}\right) - 1\right)\right)}{\exp\left(\left(-\frac{k_f^0 k_B T}{r x_f}\right) - 1\right)} \tag{3.16}$$

Normalized distributions of the unfolding and refolding forces of a molecule manipulated at constant loading rate can be fit to Eqs. (3.15) and (3.16) to estimate rate constants at zero force (k_u^0, k_f^0) and distances to the transition state (x_u, x_f) (Heidarsson et al., 2012; Schlierf, Li, & Fernandez, 2004).

Often, however, experimental force distributions are analyzed with a slightly different method. When $\exp(F x_u / k_B T) > 10$, which is usually the case with biomolecules, Eq. (3.13) can be written as

$$\ln\{P_f(F)\} = -\frac{k_u^0 k_B T}{r x_u}\left(\exp\left(\frac{F x_u}{k_B T}\right)\right) \tag{3.17}$$

which can then be linearized as

$$\ln\left\{r \ln\left(\frac{1}{P_f(F)}\right)\right\} = \ln\frac{k_u^0 k_B T}{x_u} + \left(\frac{x_u}{k_B T}\right)F \tag{3.18}$$

Through similar considerations, for the refolding process, we have

$$\ln\left\{-r \ln\left(\frac{1}{P_u(F)}\right)\right\} = \ln\frac{k_f^0 k_B T}{x_f} + \left(\frac{x_f}{k_B T}\right)F \tag{3.19}$$

Equations (3.18) and (3.19) are often used to fit $\ln[r \ln[1/N]]$ and $\ln[-r \ln[1/U]]$ versus force graphs, where N and U are the folded and unfolded fractions, respectively, which are calculated by integrating the histograms of the force distributions over the corresponding range of forces (Heidarsson et al., 2012; Li et al., 2006; Liphardt et al., 2001).

3.4. Extracting thermodynamic parameters from nonequilibrium measurements

When the rate at which force is applied on a molecule is faster than its slowest relaxation rate, the unfolding and refolding processes occur out of equilibrium. Under these experimental conditions, the free-energy change of the process is not equal to the work done on the molecule, and cannot be calculated as the area under the unfolding/refolding transitions. However, fluctuation theorems have been developed to extract equilibrium information from nonequilibrium measurements (Jarzynski, 2011). The first of these theorems to be successfully applied to single-molecule experimental data was presented by Jarzynski (1997). He derived an equality that relates the free-energy difference $\Delta G(z)$, separating states of a system at positions 0 and z along a reaction coordinate, to the work done to irreversibly switch the system between the two states:

$$\exp[-\beta \Delta G(z)] = \lim N_{N\_\infty} \langle \exp[-\beta w_i(z,r)] \rangle N \tag{3.20}$$

where $\langle\rangle$ denotes averaging over N work trajectories, $w_i(z,r)$ represents the work of the ith of N trajectories, and r is the switching rate. The first application of this method in single-molecule force spectroscopy was reported by Liphardt, Dumont, Smith, Tinoco, and Bustamante (2002). They manipulated a P5ab RNA hairpin out of equilibrium with optical tweezers and applied Jarzynski's equality to the irreversible work trajectories to extract the unfolding free energy of the molecule. Although effective for near-equilibrium processes like that observed for the P5ab RNA hairpin, in far from equilibrium systems Jarzynski's equality is hampered by large statistical uncertainties due to the exponential averaging of low work values (Gore, Ritort, & Bustamante, 2003).These large uncertainties can be significantly reduced by using Crooks' fluctuation theorem (CFT). CFT relates the amount of work done on a molecule that unfolds and refolds out of equilibrium, with the free-energy change of the process (Crooks, 1999).

Let $P_U(W)$ and $P_R(W)$ denote the probability distributions of the work performed on a molecule that is pulled (U) and relaxed (R) an infinite number times. The CFT then predicts that

$$\frac{P_U(W)}{P_R(W)} = \exp\left(\frac{W - \Delta G}{k_B T}\right) \tag{3.21}$$

where ΔG is the free-energy change between the final and the initial states of the molecule, and thus equal to the reversible work associated with this process. The value of ΔG can be determined as the point of intersection of the unfolding and refolding work distributions, where $W = \Delta G$ (Fig. 3.5). When the overlapping region of the two distributions is small because the unfolding/refolding process occurs very far from equilibrium, Bennett's acceptance ratio method (Bennett, 1976) is often used to reduce the uncertainty in the estimation of ΔG. CFT has already been applied in several single-molecule manipulation studies, as in Collin et al. (2005), Gebhardt et al. (2010), and Shank, Cecconi, Dill, Marqusee, and Bustamante (2010).

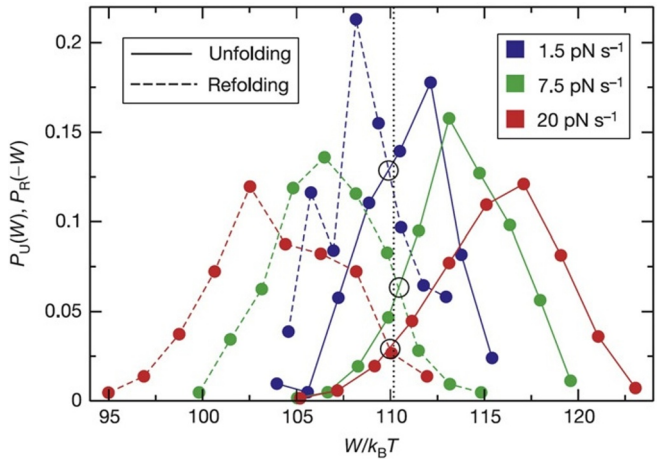

Figure 3.5 Work distributions $P_U(W)$ and $P_R(W)$ for RNA unfolding (solid curve) and refolding (dash curve) at different loading rates. The point of intersection of the two distributions gives $\Delta G = 110.3\ k_BT$. *Adapted from Collin et al. (2005) with permission.*

3.5. Extracting kinetics and thermodynamic parameters from equilibrium fluctuations

As discussed above, in constant-force and passive-mode measurements some molecules can be observed to fluctuate at equilibrium between different molecular conformations (Fig. 3.2B). Although different theoretical approaches could be used, hidden Markov models (HMMs) are often the methods of choice to extract kinetics and thermodynamic information from these experimental data (Alemany, Mossa, Junier, & Ritort, 2012; Elms, Chodera, Bustamante, & Marqusee, 2012a; Gao et al., 2011; Kaiser, Goldman, Chodera, Tinoco, & Bustamante, 2011; Stigler, Ziegler, Gieseke, Gebhardt, & Rief, 2011). HMMs are powerful statistical tools introduced by Baum and colleagues in the late 1960s and early 1970s (Baum, 1972; Baum & Petrie, 1966), and were later implemented for speech processing applications by Baker (1975). Figure 3.6 shows a general HMM, where the X_i represents the hidden state sequence, O_i the observation sequence, and A and B are the matrices of state transition and observation probabilities, respectively. HMM predicts the most likely state sequence X_i which has the maximum probability to give the observation sequence O_i by constructing a model using A and B matrices (Stamp & Le, 2005).

In the analysis of single-molecule force spectroscopy data, the HMM assumes that the observation sequence (force or extension trace) is generated by a Markov process in which the molecule makes history-independent transitions governed by a transition matrix among its different conformational states. At a given force, each state of a molecule can be defined by the distribution of extension or force values. The HMM analysis provides the transition probability matrix T that can be used to calculate the matrix for rate constants K using the relation $T = \exp(K\Delta t)$, where Δt is the data acquisition time (Chodera & Noe, 2010). Using this method, rate constants can be calculated at different forces (F) and plots of ln k versus F can be fit

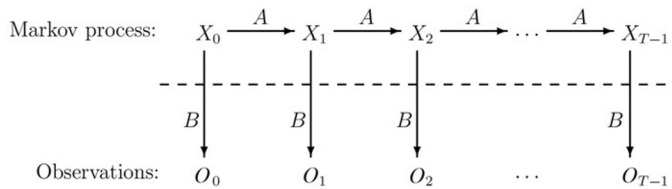

Figure 3.6 A general HMM where the hidden state sequence X_i is related to the observation sequence O_i by observation probability matrix B and transition probability matrix A. *With kind permission of Springer Science+Business Media (Stamp & Le, 2005).*

to linearized forms of Eqs. (3.8) and (3.9) to estimate the distances to the transition state and the rate constants at zero force. The ratio of the rate constants (K_{eq}) will provide information about the free energy of the reaction according to Eq. (3.4).

We would like to point out that the list of theoretical models presented above is by no means comprehensive. With the advent of new experimental strategies, novel theoretical models have also been developed and applied to different systems, as in Dudko et al. (2011), Dudko, Hummer, and Szabo (2008), Mossa, Huguet, and Ritort (2010), and Zoldak and Rief (2013).

4. BIOLOGICAL APPLICATIONS

4.1. Mechanical processes in the cell

A wide variety of cellular processes involves molecules that generate or are subjected to mechanical forces (Bustamante et al., 2004). Molecular motors such as kinesin convert chemical energy into mechanical work and movement, usually through ATP hydrolysis (Kolomeisky & Fisher, 2007). Mechanosensors go through subtle conformational changes in response to mechanical stimuli to initiate signaling cascades (Jaalouk & Lammerding, 2009). Proteins can also be unfolded by force, for example, by translocases, to target them for degradation or transport across membranes (King, Deshaies, Peters, & Kirschner, 1996; Maillard et al., 2011). Conversely, proteins perform work, and thus measurable force, through the compacting of their polypeptide chains during spontaneous folding. Below, we describe some recent studies on the conformational dynamics involved in protein folding and protein–ligand or protein–protein interactions.

4.2. Protein folding

Folding into a three-dimensional form is pivotal for the function and specificity of most proteins. The early classical experiments of Christian B. Anfinsen showed that a protein can spontaneously fold into thermodynamically stable states *in vitro* and that all the necessary information for the process is encoded in the amino acid sequence (Anfinsen, Haber, Sela, & White, 1961). Far from being a simple task, especially in the case of larger and of multidomain proteins, the mechanism of protein folding has been studied extensively over many decades. Yet, our understanding of this complex process is still incomplete. Proteins fold within a biologically relevant timescale

of microseconds to seconds despite the astronomical amount of conformations available to them, a paradox so famously stated by Cyrus Levinthal (Levinthal, 1968; Zwanzig, Szabo, & Bagchi, 1992). The paradox, which highlights the fact that protein folding would be impossible with a random search through conformational space, ultimately through simplified models and pathways, led to the idea of folding funnels (Bryngelson, Onuchic, Socci, & Wolynes, 1995; Dill & Chan, 1997; Dill & MacCallum 2012; Leopold, Montal, & Onuchic, 1992; Oliveberg & Wolynes, 2005). In this view, the folding of protein molecules is described as diffusion of a statistical ensemble over a funnel-shaped energy landscape with possibly numerous parallel pathways (Fig. 3.7A) (Dill & Chan, 1997; Onuchic, Luthey-Schulten, & Wolynes, 1997).

The funnel shape provides an energetic bias toward folding into the native state and this can be described with two seemingly counteracting properties: a decrease in (1) configurational entropy (which is unfavorable) and (2) potential energy (which is favorable) (Karplus, 2011). The funneled energy landscape contains all the information to describe the path a protein can take en route to its native state. Theory predicts that a rugged energy landscape, with many small minima, will lead to slower folding

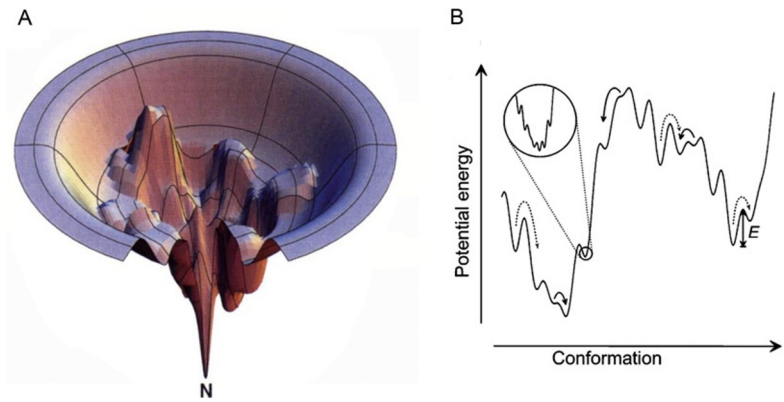

Figure 3.7 The funnel-shaped energy landscape for protein folding. (A) Proteins are currently thought to fold to their native state by diffusion over a multidimensional funnel-shaped energy landscape. (B) Two-dimensional scheme of the ruggedness of an energy landscape. Two main conformations are accessible with multiple smaller kinetic traps that are either short-lived (solid arrows) or long-lived (dotted arrows) conformations. *E* represents the height of the activation barrier for one such conformation. *(A) Adapted from Dill and Chan (1997) with permission. (B) Adapted from Milanesi et al. (2012) with permission.*

(Fig. 3.7B) and this was recently demonstrated experimentally with spectrin domains (Bryngelson & Wolynes, 1989; Wensley et al., 2010). The ensemble view suggests that due to the ruggedness of the energy landscape, a fraction of the molecules will fold slowly, due to trapping in energy minima, while other molecules will fold fast without populating intermediate states. This phenomenon is known as kinetic partitioning and explains the multiphasic kinetics observed in many systems (Thirumalai, Klimov, & Woodson, 1997). Kinetically trapped intermediate structures visited along a folding trajectory may be on-pathway, and thus productive toward the native state, or off-pathway misfolded states, which can form aggregates and lead to serious diseases (see section 4.2.3).

Traditional bulk techniques, such as NMR and protein engineering phi-value analysis (Matouschek, Kellis, Serrano, & Fersht, 1989), have unlocked a wealth of knowledge on the folding process but these methods are limited by an ensemble-averaged experimental output. Computational approaches to folding have also significantly enhanced our understanding but despite recent reports of millisecond-long simulations (Shaw et al., 2010) they have mostly been limited to probing a relatively short timescale using small, fast-folding proteins (Scheraga, Khalili, & Liwo, 2007). Single-molecule mechanical manipulation methods have added a new dimension to protein folding studies. The early mechanical manipulation instruments were only able to directly detect the unfolding process of single molecules, leaving the refolding process silent. The first of these experiments were performed simultaneously with AFM and optical tweezers on the giant muscle protein titin (Kellermayer, Smith, Granzier, & Bustamante, 1997; Rief, Gautel, Oesterhelt, Fernandez, & Gaub, 1997; Tskhovrebova, Trinick, Sleep, & Simmons, 1997). Quickly the field developed and the refolding of a single molecule into its native state was observed (Cecconi et al., 2005; Fernandez & Li, 2004). In the following years came a surge of exciting results, establishing single-molecule force spectroscopy, often in combination with molecular dynamics (MD) simulations, as a powerful tool to study protein folding.

4.2.1 Folding pathways and the energy landscape

Statistical ensemble views of protein folding predict that a rapid hydrophobic collapse into a subset of globular, unspecific structures, is the initial and necessary reduction in a polypeptide's available conformational space. This collapse has been difficult to study from the bulk viewpoint due to the averaging of pathways and ensembles (Agashe, Shastry, & Udgaonkar, 1995;

Dasgupta & Udgaonkar, 2010). AFM constant-force mode was used to study the early events of folding of individual ubiquitin molecules, induced by rapid force quenching (Garcia-Manyes et al., 2009). Garcia-Manyes et al. were able to directly observe a collapse into an ensemble of lower energy structures for ubiquitin prior to folding into the native state. Polyubiquitin molecules were first unfolded followed by quenching to low force, allowing the molecules to refold. Subsequently, the molecules were unfolded again to monitor whether the proteins had folded into their native state. The natively folded ubiquitin molecules unfolded in discrete steps but structures apparently collapsed during refolding, unfolded in various size steps and had less mechanical stability. By varying the refolding time, they were able to extract the kinetics of the refolding process and showed that the collapsed states folded in a fast phase followed by a slower phase involving a barrier-separated two-state mechanism.

The presence of multiple pathways is implied in the three-dimensional funnel-shaped energy landscape but experimental evidence for this phenomenon has remained limited (Radford, Dobson, & Evans, 1992; Wright, Lindorff-Larsen, Randles, & Clarke, 2003). This is in part due to differential populations of pathways, where some pathways may be rarely visited by a protein. He et al. studied a slipknot protein by combining AFM and course-grained Steered Molecular Dynamics (SMD) simulations (He, Genchev, Lu, & Li, 2012). They found that the protein could untie the slipknot and unfold through either a two-state or a three-state mechanism, suggesting parallel pathways. SMD simulations revealed that the intermediate state in the three-state pathway was formed only if the unfolding initiated from the C-terminus and key structural elements were found that prevent the formation of a tightened knot structure in both pathways. The results support the idea of kinetic partitioning and thus add to a growing number of evidence, suggesting it to be a general mechanism in protein folding.

Force acts on proteins locally in contrast to the global effect of temperature and chemicals. Furthermore, during mechanical manipulation, the molecule is tethered, restraining its conformational flexibility. Certainly the unfolded state in these experiments is stretched as opposed to a random coil for freely diffusing molecules. A question therefore arises on whether the folding pathways are the same when determined with chemical/thermal denaturants or with force. Originally, both experimental and computational studies suggested that force-induced unfolding differs from that induced by chemical/thermal denaturants (Best et al., 2003; Ng et al., 2005). Recently,

however, evidence has emerged for similar pathways to exist. Simulations have suggested that at sufficiently low pulling speeds, where the molecule is able to sample a large part of its conformational space, mechanical unfolding pathways may start to resemble those observed in chemical denaturation studies (West, Olmsted, & Paci, 2006). A force-induced pathway-switch has indeed recently been observed experimentally for an SH3 domain in the low-force regime using optical tweezers (Jagannathan, Elms, Bustamante, & Marqusee, 2012). Here, two different pulling axes were tested and one of them revealed two distinct and parallel unfolding pathways, giving evidence of a multidimensional energy landscape. Using both constant-velocity experiments at different velocities and force-jump experiments, the authors determined the unfolding rates for both pulling axes. Although the absolute unfolding rates determined in bulk and using mechanical manipulation cannot generally be compared (due to contributions from the DNA handles and beads, however, a very recent study reports a data analysis method that accounts for these effects (Hinczewski, Gebhardt, Rief, & Thirumalai, 2013)), the effects of mutations on the rates could be compared in this study. The rates analysis indicated that the transition states in bulk and on the single-molecule level were populated to a similar extent, suggesting similar pathways.

Similar mechanical and chemical denaturation pathways have been suggested for acyl-CoA binding protein (ACBP) (Heidarsson et al., 2012). The structure and position along the reaction coordinate of the transition state of this small globular single-domain protein were investigated using a combination of optical tweezers and ratcheted MD simulations. Through both equilibrium and nonequilibrium optical tweezers experiments, Heidarsson et al. determined the "mechanical" Tanford β-value ($m\beta_T$), which is analogous to a Tanford β-value in bulk studies (Elms et al., 2012a; Tanford, 1970). This value, which takes values between 0 and 1, can be regarded as a measure of the nativeness of the transition state and the determined $m\beta_T$ value for ACBP was very similar to the β-value in bulk (Kragelund et al., 1996). An almost identical $m\beta_T$ value was also confirmed by ratcheted MD simulations, which were then used to estimate the structure of the transition state in atomic detail. The structure resembled the structure observed in bulk through phi-value analysis and NMR chemical shifts (Bruun, Iesmantavicius, Danielsson, & Poulsen, 2010; Kragelund et al., 1999). It may therefore be protein-specific whether mechanical and chemical/thermal transition states and unfolding pathways are similar or not.

Related to transition states is the transition path, which is the seemingly instantaneous transition across the transition state barrier and includes all the

mechanistic details of how a process happens. Transition path times, the actual time it takes to cross the barrier (not to be confused with transition rates which describe the frequency of barrier crossing), are impossible to measure by bulk methods as this is entirely a single-molecule property. Yu et al. characterized the energy landscape of prion protein using optical tweezers (Yu, Gupta, et al., 2012). From constant-force experiments they reconstructed a detailed free-energy landscape and, using Kramers theory of barrier-limited diffusion, were able to directly determine the transition path times and folding rates. They found, in accordance with results from single-molecule fluorescence and MD results (Chung, McHale, Louis, & Eaton, 2012; Shaw et al., 2010), that transition path times are in the order of $\sim$2 μs. Importantly, given the size of the prion protein, this study reiterated that transition path times are relatively insensitive to protein size, whereas folding rates can vary by many orders of magnitude.

4.2.2 Molecular response to force, secondary structure, and topology

A remarkable feature of mechanical manipulation techniques is the ability to probe folding using various reaction coordinates. Almost any pulling geometry can be chosen by changing the position of the residues that define the load application. This offers the unique opportunity to directly explore the anisotropy of the energy landscape. Carrion-Vazquez et al. were the first to exploit this and using AFM they found that the direction of force application can dramatically change the mechanical stability of ubiquitin molecules (Carrion-Vazquez et al., 2003). Similar energy landscape anisotropy has been demonstrated with the green fluorescent protein (GFP) (Dietz, Berkemeier, et al., 2006). Dietz et al. performed AFM experiments on GFP using five different pulling geometries by varying the placement of cysteine residues that serve as attachment points in the polyprotein constructs (Fig. 3.8A). The mechanical stability of GFP displayed large variability, depending on the pulling axis. From the resulting unfolding force distributions (Fig. 3.8B) and using Monte Carlo simulations, the height of the transition state barriers and the potential energy well width of the native state could be determined. Remarkably, whereas the unfolding rates were not significantly affected by pulling direction, the width of the potential energy well showed significant variation, indicating either brittle or compliant behavior, depending on the pulling geometry. Ultimately, the authors were able to describe the GFP structure in terms of different directional spring constants (Fig. 3.8C), highlighting the anisotropic nature of its energy landscape. These and similar studies demonstrate how directional control can

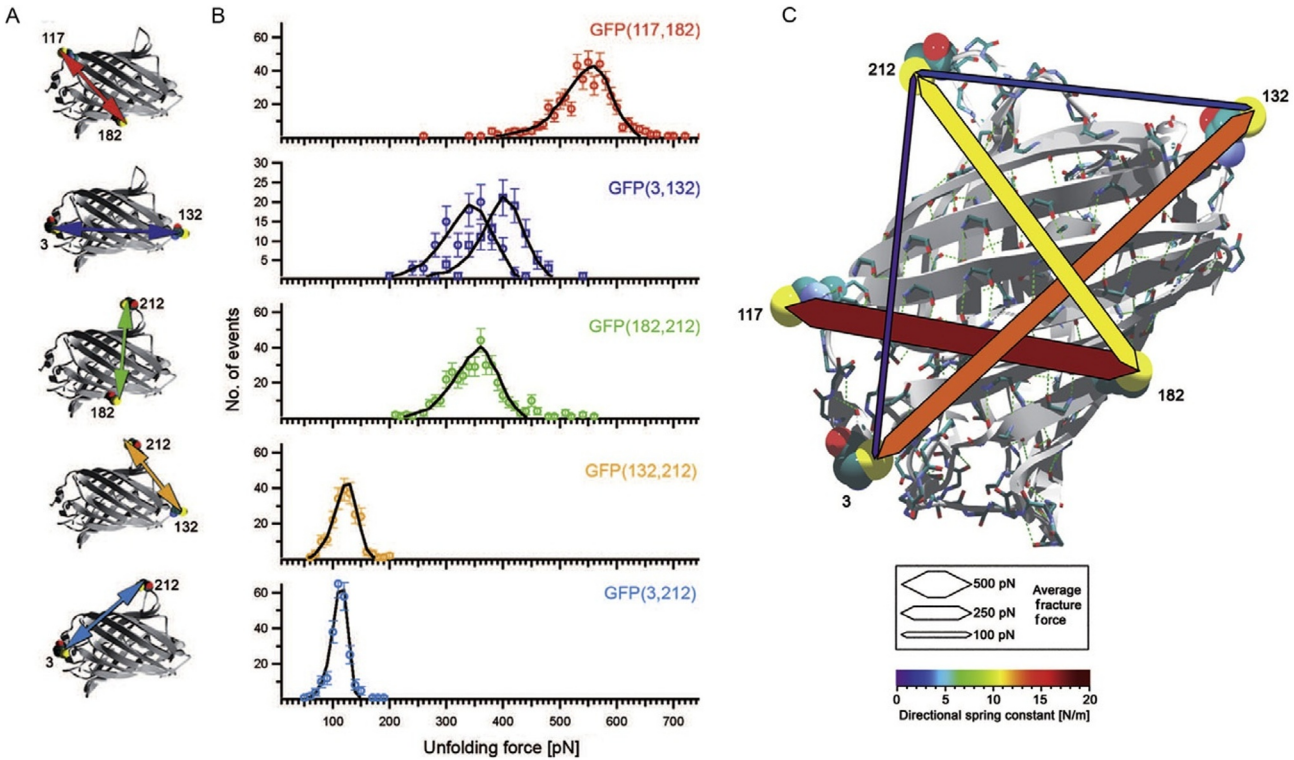

Figure 3.8 The anisotropy of GFP energy landscape probed with AFM. (A) Five different pulling geometries of GFP were studied by generating polyproteins with various attachment points through cysteine mutations. The numbers correspond to the cysteine residues and the arrows show the pulling axis. (B) Unfolding force distributions of the different variants. The solid lines represent results of a Monte Carlo simulation to reproduce the experimental data. (C) Mechanical stability (indicated by the width of arrows) and directional spring constants of GFP (indicated by the color of arrows). *Adapted from Dietz, Berkemeier, et al. (2006) with permission.*

allow exploration of regions of the energy landscape that are inaccessible to conventional methods.

The determinants of anisotropic mechanical response are likely to be encoded in the structural architecture of proteins, involving features such as secondary structure, topology, and long-range contacts. It has been demonstrated that the mechanical stability of proteins is highly dependent on secondary structure. Proteins consisting mainly of β-sheets are better able to resist mechanical denaturation than α-helical proteins, and this has been attributed to the extensive network of hydrogen bonding in β-sheet proteins in contrast to mainly hydrophobic interactions between helices (Brockwell et al., 2005; Schlierf & Rief, 2005). Secondary structure also correlates with the distance from the native state to the transition state (x_u), where helical proteins have larger distances indicating softer, more compliant structures (Li, 2007).

Topology, the arrangement of secondary elements along the sequence, has been shown to be important for cooperative folding during mechanical manipulation experiments. In T4 lysozyme (T4L), the A-helix is at the amino-terminal end but is part of the C-terminal structural domain. Shank et al. generated a circular permutant of T4L, effectively placing the A-helix at the C-terminal, and performed constant-velocity experiments using optical tweezers (Shank et al., 2010). Even though the experiments provided only nonequilibrium information, equilibrium properties of the system could be revealed using CFT (see section 3.4). In traditional ensemble studies, T4L unfolds in a single cooperative transition and this was also observed for the wild-type protein in constant-velocity experiments. However, the circular permutant displayed a three-state mechanism in which the N-domain now unfolded before the C-domain, indicating a decoupling of the two domains, which reduced cooperativity.

The mechanical properties of partially folded intermediate states are particularly interesting. Molten-globule intermediate states have significant native-like secondary structure but lack the characteristic stable tertiary interactions of the native state. Elms et al. studied the molten-globular state of apomyoglobin using optical tweezers (Elms et al., 2012a). They found that compared to native states, the molten globule is highly deformable (compliant), rendering its unfolding rate more sensitive to force, and speculated that this may be a general feature of molten globules. Surprisingly, the native state of ACBP has been shown to be even more deformable than the molten globule of apomyoglobin, a feature that may be important for its function as a lipid transporter (Heidarsson et al., 2012). The possibility that

some intermediate states and even some proteins are more sensitive to force than others implies also that nature may have evolved this feature into proteins so that cells use less energy to unfold proteins that are targeted for degradation or translocation.

4.2.3 Intermediate states, misfolded states, and beyond

The role of intermediate states in protein folding has been debated and whether they are productive to the native state has remained an open question. Cecconi et al. used optical tweezers to characterize the refolding of ribonuclease H (RNase H) (Cecconi et al., 2005). RNase H has been suggested to refold through a molten-globular intermediate state but it was unclear whether this state was on- or off-pathway (Raschke, Kho, & Marqusee, 1999). By using constant-force experiments, they observed that within a narrow range of forces the molecule "hopped" between the unfolded state and the intermediate state. In some cases, the hopping came to an abrupt stop followed by a further compaction into the native state. This compaction occurred in the vast majority of cases directly from the intermediate state, providing direct evidence that it was on-pathway to the native state.

Predicted intermediate states have also been confirmed using force spectroscopy. Soluble *N*-ethylmaleimide-sensitive factor attachment protein receptor (SNARE) proteins mediate membrane fusion and are particularly important in vesicle fusion for neurotransmitter release (Ramakrishnan, Drescher, & Drescher, 2012). Different SNARE proteins, attached to the vesicle membrane and the plasma membrane, are thought to assemble into a parallel four-helix bundle and it has been suggested that the bundle then zippers toward the membrane, producing sufficient force to enable fusion. The zippering action has, however, not been supported by direct evidence and the assembly intermediates have eluded detection. Using optical tweezers and some clever protein engineering, Gao et al. showed that a neuronal SNARE complex zippers in three distinct stages (Gao et al., 2012). By applying forces in the same range as occurs during fusion, they were able to stabilize a half-zippered intermediate. The proposed zippering mechanism spawned from this study significantly impacts the study of neurotransmitter release.

Protein folding mechanisms have not evolved to perfection and can sometimes lead to incorrectly folded states. Misfolded proteins have attracted significant attention due to their well-established link to many severe diseases such as Alzheimer's, Parkinson's, and Creutzfeldt–Jakobs' (Dobson,

2003). As the prime cause of the latter, the infectious form of the prion protein is one of the most widely studied misfolding systems. Yu et al. studied the prion protein using optical tweezers and found that folding occurred in a two-state mechanism, contrary to previous reports. They observed that besides the native state, three distinct short-lived misfolded states were also populated (Fig. 3.9A) (Yu, Liu, et al., 2012). These states were only accessible from the unfolded state, and could thus be classified as off-pathway, and remarkably, they were more frequently accessed than the native state under tension. A mutant that had higher aggregation propensity in bulk, populated two of the three misfolded states more frequently. The results of this study challenge the assumption that an on-pathway intermediate is responsible for aggregation and suggest that prion misfolding is mediated from the unfolded state, not the native state (Fig. 3.9B).

Interestingly, proteins not directly linked to misfolding diseases have been shown to populate misfolded states. The ubiquitously expressed protein calmodulin (CaM) transduces changing levels in intracellular Ca^{2+} concentrations and is one of the most extensively studied calcium binding proteins. Despite extensive information on CaM structural states and complex formations from traditional methods, single-molecule methods have been able to impressively mine new features of its folding mechanism. Besides characterizing in detail the folding network of four distinct on-pathway states, Stigler et al. observed two additional misfolded states that were the result of incorrect pairing of EF-hands (Stigler et al., 2011). This misfolding slowed the overall folding kinetics of otherwise fast-folding individual domains.

Nonnative interactions are not necessarily unwanted as elegantly demonstrated by Forman et al. (2009). The mechanosensory polycystin-1 PKD domain has been shown to be mechanically stronger than its native state predicts and MD simulations had suggested that this is due to a rearrangement leading to nonnative hydrogen bonds that resist unfolding. Using genetic engineering, the authors produced mutant proteins that were designed to prevent formation of these nonnative bonds. They subsequently showed through AFM experiments and MD simulations that, despite having a negligible effect on the native state stability, the mutations caused dramatic mechanical destabilization. Thus, formation of nonnative interactions during the mechanical unfolding of the PKD domain seems crucial for mechanical stability and, by inference, mechanosensory function.

Functional nonnative interactions have also been suggested for coiled coils, molecules that have various roles in the cell often connected with

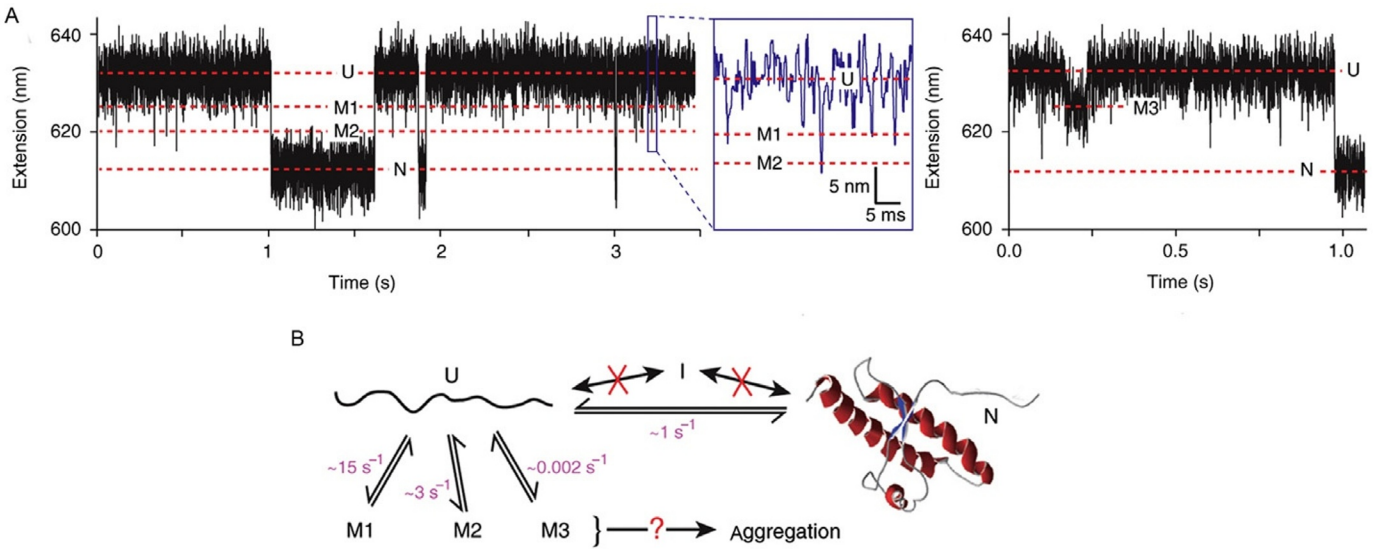

Figure 3.9 Misfolded states in single-molecule experiments. (A) Extension versus time traces of the prion protein. Left panel: the unfolded state frequently transitions into two distinct and short-lived misfolded states, M1 and M2. The inset shows a zoom into the region defined by the blue square. Right panel: rarely, a third and longer-lived misfolded state was populated. (B) An illustration of the folding/misfolding scheme of the prion protein along with the transition rates to the different misfolded states under tension. *Adapted from Yu, Liu, et al. (2012) with permission.*

sensing or generating force. The coiled coils have characteristic *abcdefg* heptad repeats that engage in the dimer interface and native coiled coil dimer formation depends on the correct pairing of the *a* and *d* positions. Sometimes, alternative pairings are formed when one helix is shifted, usually by one heptad repeat, and coiled coils have been suggested to undergo helix sliding to populate these so-called staggered helices. The nonnative conformations may be important for biological function but have eluded detailed characterization due to their instability. Using high-resolution optical tweezers, Xi et al. studied two very stable coiled coils: a variant of the GCN4 leucine zipper (pIL) and a heterodimeric coiled coil (pER) (Xi et al., 2012). The authors were able to directly observe partially folded states where the difference in the number of folded residues suggested these states to correspond to one helix shifted by one to three heptad repeats or, in other words, staggered helices. These states were populated less than 2% of the time with lifetimes decreasing inversely with the number of shifted heptad repeats. Usually, the partially folded states would only be accessed from the unfolded state (misfolding) but occasionally (<10%) the native state would transit directly into these states, which the authors interpreted as evidence for helix sliding.

Protein folding studies have greatly benefited from the advent of single-molecule manipulation studies from which new and exciting information continues to emerge. Kinetic partitioning seems to emerge as a general feature of protein folding kinetics and the frequent observation of misfolded states, even in small proteins thought to be efficient folders, challenges the idea of a highly evolved folding process. However, the traditional focus of protein folding studies needs to broaden from mostly single-domain proteins to more complex systems, as only a handful of larger proteins and double-domain systems has been explored on the single-molecule level. The current development of novel and hybrid instruments promises the ability to tackle ever more complex proteins and determine the details of multidomain protein folding.

4.3. Protein–ligand and protein–protein interactions

Proteins interact with a multitude of binding partners *in vivo* and these interactions naturally affect their structure and energetics. Molecular chaperones interact with proteins to improve the fidelity of their folding process, sometimes by rescuing misfolded states (Hartl, Bracher, & Hayer-Hartl, 2011). The binding of various ions can activate proteins

by inducing conformational change, such as in the case of calcium sensors, to initiate signaling pathways (Chazin, 2011). Conformational dynamics and flexibility are the hallmark of protein interactions (Teilum, Olsen, & Kragelund, 2011) and single-molecule force spectroscopy is now being used to probe these events in significant detail.

Mechanical stability is largely governed by specific noncovalent interactions in the protein and ligand binding can induce conformational changes in the protein structure that lead to changes in mechanical stability. Alterations in mechanical stability upon ligand binding can therefore serve as an intrinsic reporter to identify the functional state of protein at the single-molecule level (Cao, Balamurali, Sharma, & Li, 2007). The effect of ligand binding on the mechanical stability of a protein is not easy to predict. Using AFM, only moderate increases in mechanical stability were observed upon ligand binding to mouse dihydrofolate reductase (DHFR) (Junker, Hell, Schlierf, Neupert, & Rief, 2005) and to Im9 (Hann et al., 2007) while strong enhancement of mechanical stability occurs when protein G interacts with an Fc fragment from IgG (Cao et al., 2007). Stabilization of enzymatically inactive conformations by inhibitors might have significant importance in biomedical applications and drug design. For instance, the role of DHFR in cell proliferation and growth has rendered this enzyme a target for anticancer drug therapy (Li et al., 2000). Through AFM experiments Ainavarapu et al. showed that binding of the cancer chemotherapeutic agent methotrexate (MTX) to DHFR increases the mechanical stability of the enzyme (Ainavarapu, Li, Badilla, & Fernandez, 2005). The correlation between this result and the decrease in the degradation rate of DHFR inside the cell supports the idea that force-induced denaturation is necessary for translocation and degradation of this protein. Also, through similar experiments, Junker et al., have shown that simultaneous binding of MTX and the cofactor NADHP to DHFR increases the lifetime of one intermediate state of the protein, suggesting that MTX and NADHP could inhibit DHFR by trapping it in an enzymatically inactive intermediate structure (Junker et al., 2005).

Several proteins, like CaM, are activated by calcium ion binding, which allows them to interact with a vast array of binding partners. Using optical tweezers, Stigler and Rief studied CaM folding under conditions approaching physiological Ca^{2+} concentrations (Stigler & Rief, 2012). Variations in Ca^{2+} concentrations led to dramatic changes in the folding/unfolding kinetics of CaM. At high Ca^{2+} concentrations, CaM folding was characterized by a complex network of on- and off-pathway intermediate states (Fig. 3.10A). At low Ca^{2+} concentrations, the folding network remained the same but the

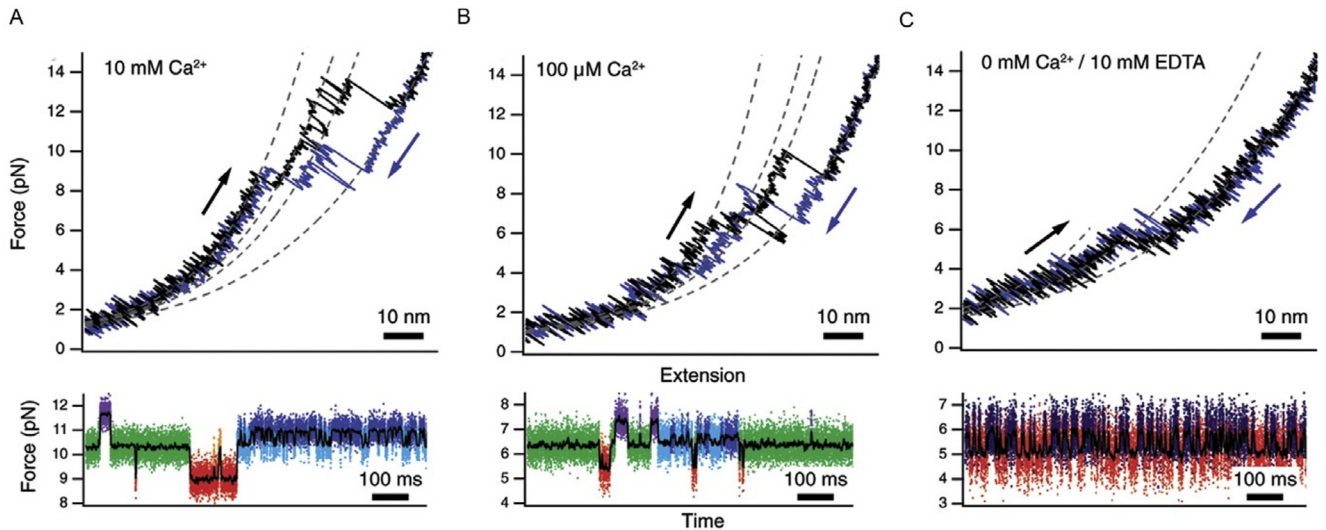

Figure 3.10 Calcium binding modulates the mechanical folding behavior of CaM. Force versus extension cycles of CaM with varying Ca^{2+} concentration. (A) 10 mM Ca^{2+}, (B) 100 µm Ca^{2+}, and (C) 0 mM Ca^{2+}. The lower panels show force versus time traces, where the two beads tethering the molecule are kept at a constant distance. At high Ca^{2+} concentrations, CaM populates four intermediate structures between the unfolded and folded states, each color-coded. At lower Ca^{2+} concentrations, the same folding pattern is observed but at low forces. Under apo-conditions (0 mM Ca^{2+}), the kinetic pattern changes drastically and CaM fluctuates between only two states. Dotted lines in upper panels represent WLC fits to the data. Arrows indicate pulling direction. *Adapted from Stigler and Rief (2012) with permission.*

mechanical stability of the protein drops and the unfolding and refolding rate constants changed significantly (Fig. 3.10B). In the absence of Ca^{2+}, the CaM folding network was essentially reduced to a two-state mechanism (Fig. 3.10C).

Chaperones interact directly with polypeptide chains to increase the efficiency of folding. Some chaperones can prevent misfolding and aggregation, or facilitate protein translocation across membranes or for degradation (Maillard et al., 2011). However, the mechanism by which folding pathways are affected by chaperones is poorly understood. Bechtluft and coworkers used optical tweezers in combination with MD simulations to study the effect of the chaperone SecB on the folding pathway of maltose binding protein (MBP) (Bechtluft et al., 2007). They observed that, in the absence of SecB, MBP populated a molten-globule-like compacted state before folding into its native structure. Upon addition, SecB binds to the molten-globule state, stabilizing it and preventing the formation of stable native tertiary contacts of MBP. The effect of SecB on the structure of MBP might explain the mechanism by which this chaperone facilitates translocation of this protein through cellular membranes, as the absence of stable tertiary contacts likely facilitates the passage of the protein through the translocation machinery. This work demonstrated how effective optical tweezers approaches can be to elucidate the effect of chaperones on protein folding landscapes.

Kim et al. developed an elegant optical tweezers method to perform repeated measurements of the binding/release kinetics between receptor and ligand (Kim, Zhang, Zhang, & Springer, 2010). Using this novel method, they were able to investigate the interaction between the A1 domain of von Willebrand factor (VWF) and the leucine-rich repeat (LRR) domain of glycoprotein Ib α subunit (GPIbα) by tethering the two molecules together via a flexible linker (Fig. 3.11A). Force experiments at different pulling rates and constant-force showed that the A1–GPIbα interaction exists in two states (Fig. 3.11B and C), which the authors referred to as a flex-bond. One state was observed at low force whereas the other was mechanically more stable and had a much longer lifetime. The kinetics of the bond formation (Fig. 3.11D) help to explain how platelets bound to VWF are able to resist force to plug arterioles and how increased flow activates platelet plug formation.

5. FUTURE PERSPECTIVES

Single-molecule methods are making an impact in many aspects of cellular and molecular biology and several new and exciting developments are on the horizon. Intrinsically disordered proteins (IDPs) are a recently

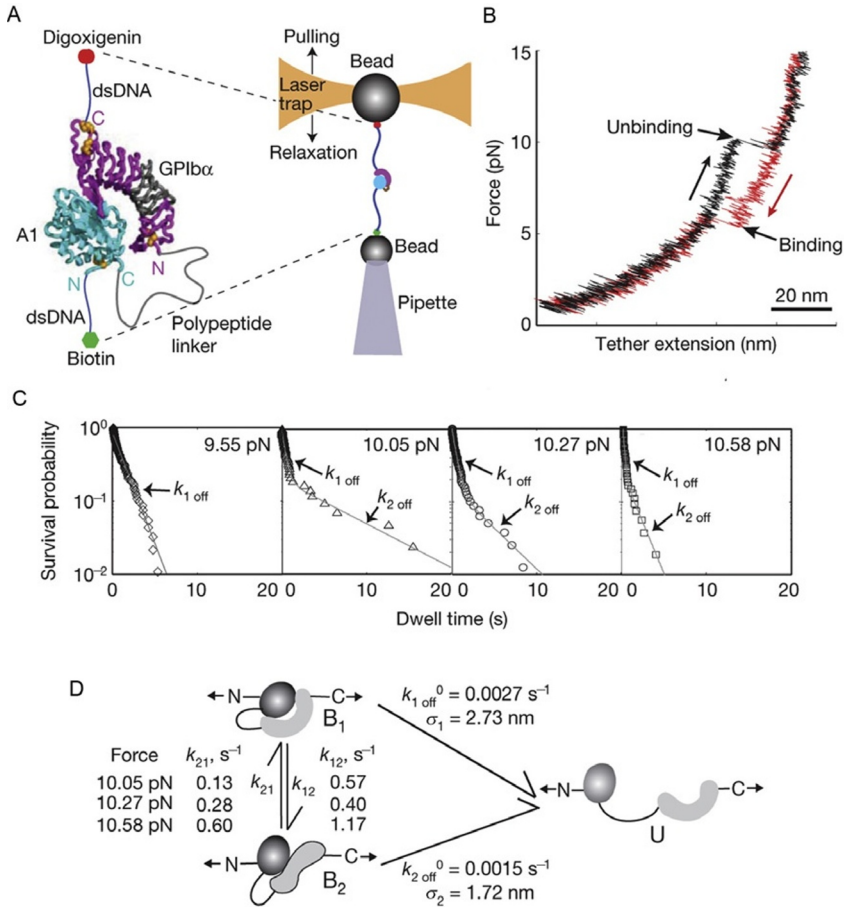

Figure 3.11 Novel approach to studying receptor–ligand binding/unbinding kinetics. (A) The experimental setup. Left: the A1 domain–GPIbα LRR domain construct. Right: the optical tweezers setup. (B) Force versus extension trace for one cycle of stretching (black) and relaxing (red). (C) Constant-force experiments were performed to determine the survival probability of the bound state as a function of time at different force values. (D) A model of the A1–GPIbα flex-bond and the associated rate constants. *Adapted from Kim et al. (2010) with permission.*

recognized group of proteins where the central paradigm of a folded functional protein is challenged (Tompa, 2011). These proteins have seemingly no defined structure, allowing significant functional plasticity but their properties are just beginning to be studied at the single-molecule level. So far, IDPs have exclusively been studied with single-molecule detection techniques but mechanical manipulation should offer an attractive approach

to tackle IDPs as well. Optical tweezers have already successfully manipulated objects in living cells (Oddershede, 2012). The dream is that near-future instrumental and methodological advances will allow us to directly observe life unfold by watching individual molecules *in vivo*, in real time.

ACKNOWLEDGMENTS

P. O. H. acknowledges the Carlsberg Foundation for financial support. C. C. gratefully acknowledges financial support from Fondazione Cassa di Risparmio di Modena, the EU through a Marie Curie International Reintegration Grant (No. 44952), the Italian MIUR (Grant No. 17DPXLNBEK), and partial support from Italian MIUR FIRB RBPR05JH2P "ITALNANONET." Dr. Birthe B. Kragelund is thanked for critical reading of parts of this manuscript.

REFERENCES

Agashe, V. R., Shastry, M. C., & Udgaonkar, J. B. (1995). Initial hydrophobic collapse in the folding of barstar. *Nature*, *377*(6551), 754–757.

Ainavarapu, S. R., Li, L., Badilla, C. L., & Fernandez, J. M. (2005). Ligand binding modulates the mechanical stability of dihydrofolate reductase. *Biophysical Journal*, *89*(5), 3337–3344.

Alemany, A., Mossa, A., Junier, I., & Ritort, F. (2012). Experimental free-energy measurements of kinetic molecular states using fluctuation theorems. *Nature Physics*, *8*, 688–694.

Anfinsen, C. B., Haber, E., Sela, M., & White, F. H., Jr. (1961). The kinetics of formation of native ribonuclease during oxidation of the reduced polypeptide chain. *Proceedings of the National Academy of Sciences of the United States of America*, *47*, 1309–1314.

Ashkin, A., Dziedzic, J. M., Bjorkholm, J. E., & Chu, S. (1986). Observation of a single-beam gradient force optical trap for dielectric particles. *Optics Letters*, *11*(5), 288–290.

Baker, J. K. (1975). The dragon system—An overview. *IEEE Transactions on Acoustics, Speech, & Signal Processing*, *23*, 24–29.

Baum, L. E. (1972). An inequality and associated maximization technique in statistical estimation for probabilistic functions of Markov processes. *Inequalities*, *3*, 1–8.

Baum, L. E., & Petrie, T. (1966). Statistical inference for probabilistic functions of finite state Markov chains. *Annals of Mathematical Statistics*, *37*, 1554–1563.

Bechtluft, P., van Leeuwen, R. G. H., Tyreman, M., Tomkiewicz, D., Nouwen, N., Tepper, H. L., et al. (2007). Direct observation of chaperone-induced changes in a protein folding pathway. *Science*, *318*(5855), 1458–1461.

Bell, G. I. (1978). Models for the specific adhesion of cells to cells. *Science*, *200*(4342), 618–627.

Bennett, C. H. (1976). Efficient estimation of free energy differences from Monte Carlo data. *Journal of Computational Physics*, *22*, 245–268.

Best, R. B., Fowler, S. B., Herrera, J. L., Steward, A., Paci, E., & Clarke, J. (2003). Mechanical unfolding of a titin Ig domain: Structure of transition state revealed by combining atomic force microscopy, protein engineering and molecular dynamics simulations. *Journal of Molecular Biology*, *330*(4), 867–877.

Binnig, G., Quate, C. F., & Gerber, C. (1986). Atomic force microscope. *Physical Review Letters*, *56*(9), 930–933.

Borgia, A., Williams, P. M., & Clarke, J. (2008). Single-molecule studies of protein folding. *Annual Review of Biochemistry*, *77*, 101–125.

Bornschlogl, T., & Rief, M. (2011). Single-molecule protein unfolding and refolding using atomic force microscopy. *Methods in Molecular Biology*, *783*, 233–250.

Brockwell, D. J., Beddard, G. S., Paci, E., West, D. K., Olmsted, P. D., Smith, D. A., et al. (2005). Mechanically unfolding the small, topologically simple protein L. *Biophysical Journal*, *89*(1), 506–519.

Bruun, S. W., Iesmantavicius, V., Danielsson, J., & Poulsen, F. M. (2010). Cooperative formation of native-like tertiary contacts in the ensemble of unfolded states of a four-helix protein. *Proceedings of the National Academy of Sciences of the United States of America*, *107*(30), 13306–13311.

Bryngelson, J. D., Onuchic, J. N., Socci, N. D., & Wolynes, P. G. (1995). Funnels, pathways, and the energy landscape of protein folding: A synthesis. *Proteins*, *21*(3), 167–195.

Bryngelson, J. D., & Wolynes, P. G. (1989). Intermediates and barrier crossing in a random energy-model (with applications to protein folding). *The Journal of Physical Chemistry*, *93*(19), 6902–6915.

Bustamante, C. (2008). In singulo biochemistry: When less is more. *Annual Review of Biochemistry*, *77*, 45–50.

Bustamante, C., Chemla, Y. R., Forde, N. R., & Izhaky, D. (2004). Mechanical processes in biochemistry. *Annual Review of Biochemistry*, *73*, 705–748.

Bustamante, C., Marko, J. F., Siggia, E. D., & Smith, S. (1994). Entropic elasticity of lambda-phage DNA. *Science*, *265*(5178), 1599–1600.

Cao, Y., Balamurali, M. M., Sharma, D., & Li, H. (2007). A functional single-molecule binding assay via force spectroscopy. *Proceedings of the National Academy of Sciences of the United States of America*, *104*(40), 15677–15681.

Carrion-Vazquez, M., Li, H., Lu, H., Marszalek, P. E., Oberhauser, A. F., & Fernandez, J. M. (2003). The mechanical stability of ubiquitin is linkage dependent. *Nature Structural Biology*, *10*(9), 738–743.

Carrion-Vazquez, M., Oberhauser, A. F., Fowler, S. B., Marszalek, P. E., Broedel, S. E., Clarke, J., et al. (1999). Mechanical and chemical unfolding of a single protein: A comparison. *Proceedings of the National Academy of Sciences of the United States of America*, *96*(7), 3694–3699.

Cecconi, C., Shank, E. A., Bustamante, C., & Marqusee, S. (2005). Direct observation of the three-state folding of a single protein molecule. *Science*, *309*(5743), 2057–2060.

Cecconi, C., Shank, E. A., Dahlquist, F. W., Marqusee, S., & Bustamante, C. (2008). Protein-DNA chimeras for single molecule mechanical folding studies with the optical tweezers. *European Biophysics Journal*, *37*(6), 729–738.

Cecconi, C., Shank, E. A., Marqusee, S., & Bustamante, C. (2011). DNA molecular handles for single-molecule protein-folding studies by optical tweezers. *Methods in Molecular Biology*, *749*, 255–271.

Chazin, W. J. (2011). Relating form and function of EF-hand calcium binding proteins. *Accounts of Chemical Research*, *44*(3), 171–179.

Chodera, J. D., & Noe, F. (2010). Probability distributions of molecular observables computed from Markov models. II. Uncertainties in observables and their time-evolution. *The Journal of Chemical Physics*, *133*(10), 105102.

Chung, H. S., McHale, K., Louis, J. M., & Eaton, W. A. (2012). Single-molecule fluorescence experiments determine protein folding transition path times. *Science*, *335*(6071), 981–984.

Collin, D., Ritort, F., Jarzynski, C., Smith, S. B., Tinoco, I., Jr., & Bustamante, C. (2005). Verification of the Crooks fluctuation theorem and recovery of RNA folding free energies. *Nature*, *437*(7056), 231–234.

Crooks, G. E. (1999). Entropy production fluctuation theorem and the nonequilibrium work relation for free energy differences. *Physical Review E: Statistical Physics, Plasmas, Fluids, and Related Interdisciplinary Topics*, *60*(3), 2721–2726.

Dame, R. T., Noom, M. C., & Wuite, G. J. (2006). Bacterial chromatin organization by H-NS protein unravelled using dual DNA manipulation. *Nature*, *444*(7117), 387–390.
Dasgupta, A., & Udgaonkar, J. B. (2010). Evidence for initial non-specific polypeptide chain collapse during the refolding of the SH3 domain of PI3 kinase. *Journal of Molecular Biology*, *403*(3), 430–445.
Deniz, A. A., Mukhopadhyay, S., & Lemke, E. A. (2008). Single-molecule biophysics: At the interface of biology, physics and chemistry. *Journal of the Royal Society Interface*, *5*(18), 15–45.
De Vlaminck, I., & Dekker, C. (2012). Recent advances in magnetic tweezers. *Annual Review of Biophysics*, *41*, 453–472.
De Vlaminck, I., Henighan, T., van Loenhout, M. T., Burnham, D. R., & Dekker, C. (2012). Magnetic forces and DNA mechanics in multiplexed magnetic tweezers. *PLoS One*, *7*(8), e41432.
De Vlaminck, I., Vidic, I., van Loenhout, M. T., Kanaar, R., Lebbink, J. H., & Dekker, C. (2010). Torsional regulation of hRPA-induced unwinding of double-stranded DNA. *Nucleic Acids Research*, *38*(12), 4133–4142.
Dietz, H., Berkemeier, F., Bertz, M., & Rief, M. (2006). Anisotropic deformation response of single protein molecules. *Proceedings of the National Academy of Sciences of the United States of America*, *103*(34), 12724–12728.
Dietz, H., Bertz, M., Schlierf, M., Berkemeier, F., Bornschlogl, T., Junker, J. P., et al. (2006). Cysteine engineering of polyproteins for single-molecule force spectroscopy. *Nature Protocols*, *1*(1), 80–84.
Dill, K. A., & Chan, H. S. (1997). From Levinthal to pathways to funnels. *Nature Structural Biology*, *4*(1), 10–19.
Dill, K. A., & MacCallum, J. L. (2012). The protein-folding problem, 50 years on. *Science*, *338*(6110), 1042–1046.
Dobson, C. M. (2003). Protein folding and misfolding. *Nature*, *426*(6968), 884–890.
Dudko, O. K., Graham, T. G., & Best, R. B. (2011). Locating the barrier for folding of single molecules under an external force. *Physical Review Letters*, *107*(20), 208301.
Dudko, O. K., Hummer, G., & Szabo, A. (2008). Theory, analysis, and interpretation of single-molecule force spectroscopy experiments. *Proceedings of the National Academy of Sciences of the United States of America*, *105*(41), 15755–15760.
Elms, P. J., Chodera, J. D., Bustamante, C., & Marqusee, S. (2012a). The molten globule state is unusually deformable under mechanical force. *Proceedings of the National Academy of Sciences of the United States of America*, *109*(10), 3796–3801.
Elms, P. J., Chodera, J. D., Bustamante, C. J., & Marqusee, S. (2012b). Limitations of constant-force-feedback experiments. *Biophysical Journal*, *103*(7), 1490–1499.
Fernandez, J. M., & Li, H. (2004). Force-clamp spectroscopy monitors the folding trajectory of a single protein. *Science*, *303*(5664), 1674–1678.
Florin, E. L., Moy, V. T., & Gaub, H. E. (1994). Adhesion forces between individual ligand-receptor pairs. *Science*, *264*(5157), 415–417.
Forman, J. R., Yew, Z. T., Qamar, S., Sandford, R. N., Paci, E., & Clarke, J. (2009). Non-native interactions are critical for mechanical strength in PKD domains. *Structure*, *17*(12), 1582–1590.
Gao, Y., Sirinakis, G., & Zhang, Y. (2011). Highly anisotropic stability and folding kinetics of a single coiled coil protein under mechanical tension. *Journal of the American Chemical Society*, *133*(32), 12749–12757.
Gao, Y., Zorman, S., Gundersen, G., Xi, Z., Ma, L., Sirinakis, G., et al. (2012). Single reconstituted neuronal SNARE complexes zipper in three distinct stages. *Science*, *337*(6100), 1340–1343.
Garcia-Manyes, S., Dougan, L., Badilla, C. L., Brujic, J., & Fernandez, J. M. (2009). Direct observation of an ensemble of stable collapsed states in the mechanical folding of

ubiquitin. *Proceedings of the National Academy of Sciences of the United States of America*, *106*(26), 10534–10539.
Gebhardt, J. C., Bornschlogl, T., & Rief, M. (2010). Full distance-resolved folding energy landscape of one single protein molecule. *Proceedings of the National Academy of Sciences of the United States of America*, *107*(5), 2013–2018.
Gore, J., Ritort, F., & Bustamante, C. (2003). Bias and error in estimates of equilibrium free-energy differences from nonequilibrium measurements. *Proceedings of the National Academy of Sciences of the United States of America*, *100*(22), 12564–12569.
Grandbois, M., Beyer, M., Rief, M., Clausen-Schaumann, H., & Gaub, H. E. (1999). How strong is a covalent bond? *Science*, *283*(5408), 1727–1730.
Greenfield, N. J. (2007). Using circular dichroism spectra to estimate protein secondary structure. *Nature Protocols*, *1*(6), 2876–2890.
Hann, E., Kirkpatrick, N., Kleanthous, C., Smith, D. A., Radford, S. E., & Brockwell, D. J. (2007). The effect of protein complexation on the mechanical stability of Im9. *Biophysical Journal*, *92*(9), L79–L81.
Hartl, F. U., Bracher, A., & Hayer-Hartl, M. (2011). Molecular chaperones in protein folding and proteostasis. *Nature*, *475*(7356), 324–332.
He, C., Genchev, G. Z., Lu, H., & Li, H. (2012). Mechanically untying a protein slipknot: Multiple pathways revealed by force spectroscopy and steered molecular dynamics simulations. *Journal of the American Chemical Society*, *134*(25), 10428–10435.
Heidarsson, P. O., Valpapuram, I., Camilloni, C., Imparato, A., Tiana, G., Poulsen, F. M., et al. (2012). A highly compliant protein native state with a spontaneous-like mechanical unfolding pathway. *Journal of the American Chemical Society*, *134*(41), 17068–17075.
Hinczewski, M., Gebhardt, J. C., Rief, M., & Thirumalai, D. (2013). From mechanical folding trajectories to intrinsic energy landscapes of biopolymers. *Proceedings of the National Academy of Sciences of the United States of America*, *110*, 4500–4505.
Jaalouk, D. E., & Lammerding, J. (2009). Mechanotransduction gone awry. *Nature Reviews. Molecular Cell Biology*, *10*(1), 63–73.
Jagannathan, B., Elms, P. J., Bustamante, C., & Marqusee, S. (2012). Direct observation of a force-induced switch in the anisotropic mechanical unfolding pathway of a protein. *Proceedings of the National Academy of Sciences of the United States of America*, *109*(44), 17820–17825.
Jarzynski, C. (1997). Nonequilibrium equality for free energy differences. *Physical Review Letters*, *78*, 2690–2693.
Jarzynski, C. (2011). Equalities and inequalities: Irreversibility and the second law of thermodynamics at the nanoscale. *Annual Reviews of Condensed Matter Physics*, *2*, 329–351.
Joo, C., Balci, H., Ishitsuka, Y., Buranachai, C., & Ha, T. (2008). Advances in single-molecule fluorescence methods for molecular biology. *Annual Review of Biochemistry*, *77*, 51–76.
Junker, J. P., Hell, K., Schlierf, M., Neupert, W., & Rief, M. (2005). Influence of substrate binding on the mechanical stability of mouse dihydrofolate reductase. *Biophysical Journal*, *89*(5), L46–L48.
Junker, J. P., & Rief, M. (2009). Single-molecule force spectroscopy distinguishes target binding modes of calmodulin. *Proceedings of the National Academy of Sciences of the United States of America*, *106*(34), 14361–14366.
Junker, J. P., Ziegler, F., & Rief, M. (2009). Ligand-dependent equilibrium fluctuations of single calmodulin molecules. *Science*, *323*(5914), 633–637.
Kaiser, C. M., Goldman, D. H., Chodera, J. D., Tinoco, I., Jr., & Bustamante, C. (2011). The ribosome modulates nascent protein folding. *Science*, *334*(6063), 1723–1727.
Karplus, M. (2011). Behind the folding funnel diagram. *Nature Chemical Biology*, *7*(7), 401–404.

Kellermayer, M. S., Smith, S. B., Granzier, H. L., & Bustamante, C. (1997). Folding-unfolding transitions in single titin molecules characterized with laser tweezers. *Science*, *276*(5315), 1112–1116.

Kern, D., Eisenmesser, E. Z., & Wolf-Watz, M. (2005). Enzyme dynamics during catalysis measured by NMR spectroscopy. *Methods in Enzymology*, *394*, 507–524.

Kim, J., Zhang, C. Z., Zhang, X., & Springer, T. A. (2010). A mechanically stabilized receptor-ligand flex-bond important in the vasculature. *Nature*, *466*(7309), 992–995.

King, R. W., Deshaies, R. J., Peters, J. M., & Kirschner, M. W. (1996). How proteolysis drives the cell cycle. *Science*, *274*(5293), 1652–1659.

Kolomeisky, A. B., & Fisher, M. E. (2007). Molecular motors: A theorist's perspective. *Annual Review of Physical Chemistry*, *58*, 675–695.

Koster, D. A., Crut, A., Shuman, S., Bjornsti, M. A., & Dekker, N. H. (2010). Cellular strategies for regulating DNA supercoiling: A single-molecule perspective. *Cell*, *142*(4), 519–530.

Kragelund, B. B., Hojrup, P., Jensen, M. S., Schjerling, C. K., Juul, E., Knudsen, J., et al. (1996). Fast and one-step folding of closely and distantly related homologous proteins of a four-helix bundle family. *Journal of Molecular Biology*, *256*(1), 187–200.

Kragelund, B. B., Osmark, P., Neergaard, T. B., Schiodt, J., Kristiansen, K., Knudsen, J., et al. (1999). The formation of a native-like structure containing eight conserved hydrophobic residues is rate limiting in two-state protein folding of ACBP. *Nature Structural Biology*, *6*(6), 594–601.

Lee, G. U., Chrisey, L. A., & Colton, R. J. (1994). Direct measurement of the forces between complementary strands of DNA. *Science*, *266*(5186), 771–773.

Leopold, P. E., Montal, M., & Onuchic, J. N. (1992). Protein folding funnels: A kinetic approach to the sequence-structure relationship. *Proceedings of the National Academy of Sciences of the United States of America*, *89*(18), 8721–8725.

Levintha, C. (1968). Are there pathways for protein folding. *Journal de Chimie Physique et de Physico-Chimie Biologique*, *65*(1), 44–45.

Li, M. S. (2007). Secondary structure, mechanical stability, and location of transition state of proteins. *Biophysical Journal*, *93*(8), 2644–2654.

Li, P. T., Collin, D., Smith, S. B., Bustamante, C., & Tinoco, I., Jr. (2006). Probing the mechanical folding kinetics of TAR RNA by hopping, force-jump, and force-ramp methods. *Biophysical Journal*, *90*(1), 250–260.

Li, R., Sirawaraporn, R., Chitnumsub, P., Sirawaraporn, W., Wooden, J., Athappilly, F., et al. (2000). Three-dimensional structure of *M. tuberculosis* dihydrofolate reductase reveals opportunities for the design of novel tuberculosis drugs. *Journal of Molecular Biology*, *295*(2), 307–323.

Liphardt, J., Dumont, S., Smith, S. B., Tinoco, I., Jr., & Bustamante, C. (2002). Equilibrium information from nonequilibrium measurements in an experimental test of Jarzynski's equality. *Science*, *296*(5574), 1832–1835.

Liphardt, J., Onoa, B., Smith, S. B., Tinoco, I., Jr., & Bustamante, C. (2001). Reversible unfolding of single RNA molecules by mechanical force. *Science*, *292*(5517), 733–737.

Maillard, R. A., Chistol, G., Sen, M., Righini, M., Tan, J., Kaiser, C. M., et al. (2011). ClpX(P) generates mechanical force to unfold and translocate its protein substrates. *Cell*, *145*(3), 459–469.

Maity, H., Maity, M., Krishna, M. M., Mayne, L., & Englander, S. W. (2005). Protein folding: The stepwise assembly of foldon units. *Proceedings of the National Academy of Sciences of the United States of America*, *102*(13), 4741–4746.

Manosas, M., Collin, D., & Ritort, F. (2006). Force-dependent fragility in RNA hairpins. *Physical Review Letters*, *96*(21), 218301.

Marszalek, P. E., Oberhauser, A. F., Pang, Y. P., & Fernandez, J. M. (1998). Polysaccharide elasticity governed by chair-boat transitions of the glucopyranose ring. *Nature*, *396*(6712), 661–664.

Matouschek, A., Kellis, J. T., Jr., Serrano, L., & Fersht, A. R. (1989). Mapping the transition state and pathway of protein folding by protein engineering. *Nature*, *340*(6229), 122–126.

Milanesi, L., Waltho, J. P., Hunter, C. A., Shaw, D. J., Beddard, G. S., Reid, G. D., et al. (2012). Measurement of energy landscape roughness of folded and unfolded proteins. *Proceedings of the National Academy of Sciences of the United States of America*, *109*(48), 19563–19568.

Moffitt, J. R., Chemla, Y. R., Smith, S. B., & Bustamante, C. (2008). Recent advances in optical tweezers. *Annual Review of Biochemistry*, *77*, 205–228.

Mossa, A., Huguet, J. M., & Ritort, F. (2010). Investigating the thermodynamics of small biosystems with optical tweezers. *Physica E: Low-dimensional Systems and Nanostructures*, *42*(3), 666–671.

Neuman, K. C., & Nagy, A. (2008). Single-molecule force spectroscopy: Optical tweezers, magnetic tweezers and atomic force microscopy. *Nature Methods*, *5*(6), 491–505.

Ng, S. P., Randles, L. G., & Clarke, J. (2007). Single molecule studies of protein folding using atomic force microscopy. *Methods in Molecular Biology*, *350*, 139–167.

Ng, S. P., Rounsevell, R. W., Steward, A., Geierhaas, C. D., Williams, P. M., Paci, E., et al. (2005). Mechanical unfolding of TNfn3: The unfolding pathway of a fnIII domain probed by protein engineering, AFM and MD simulation. *Journal of Molecular Biology*, *350*(4), 776–789.

Noom, M. C., van den Broek, B., van Mameren, J., & Wuite, G. J. (2007). Visualizing single DNA-bound proteins using DNA as a scanning probe. *Nature Methods*, *4*(12), 1031–1036.

Oddershede, L. B. (2012). Force probing of individual molecules inside the living cell is now a reality. *Nature Chemical Biology*, *8*(11), 879–886.

Oliveberg, M., & Wolynes, P. G. (2005). The experimental survey of protein-folding energy landscapes. *Quarterly Reviews of Biophysics*, *38*(3), 245–288.

Onuchic, J. N., Luthey-Schulten, Z., & Wolynes, P. G. (1997). Theory of protein folding: The energy landscape perspective. *Annual Review of Physical Chemistry*, *48*, 545–600.

Raab, A., Han, W., Badt, D., Smith-Gill, S. J., Lindsay, S. M., Schindler, H., et al. (1999). Antibody recognition imaging by force microscopy. *Nature Biotechnology*, *17*(9), 901–905.

Radford, S. E., Dobson, C. M., & Evans, P. A. (1992). The folding of hen lysozyme involves partially structured intermediates and multiple pathways. *Nature*, *358*(6384), 302–307.

Ramakrishnan, N. A., Drescher, M. J., & Drescher, D. G. (2012). The SNARE complex in neuronal and sensory cells. *Molecular and Cellular Neurosciences*, *50*(1), 58–69.

Raschke, T. M., Kho, J., & Marqusee, S. (1999). Confirmation of the hierarchical folding of RNase H: A protein engineering study. *Nature Structural Biology*, *6*(9), 825–831.

Rief, M., Gautel, M., Oesterhelt, F., Fernandez, J. M., & Gaub, H. E. (1997). Reversible unfolding of individual titin immunoglobulin domains by AFM. *Science*, *276*(5315), 1109–1112.

Rief, M., Oesterhelt, F., Heymann, B., & Gaub, H. E. (1997). Single molecule force spectroscopy on polysaccharides by atomic force microscopy. *Science*, *275*(5304), 1295–1297.

Rounsevell, R., Forman, J. R., & Clarke, J. (2004). Atomic force microscopy: Mechanical unfolding of proteins. *Methods*, *34*(1), 100–111.

Scheraga, H. A., Khalili, M., & Liwo, A. (2007). Protein-folding dynamics: Overview of molecular simulation techniques. *Annual Review of Physical Chemistry*, *58*, 57–83.

Schlierf, M., Berkemeier, F., & Rief, M. (2007). Direct observation of active protein folding using lock-in force spectroscopy. *Biophysical Journal*, *93*(11), 3989–3998.
Schlierf, M., Li, H., & Fernandez, J. M. (2004). The unfolding kinetics of ubiquitin captured with single-molecule force-clamp techniques. *Proceedings of the National Academy of Sciences of the United States of America*, *101*(19), 7299–7304.
Schlierf, M., & Rief, M. (2005). Temperature softening of a protein in single-molecule experiments. *Journal of Molecular Biology*, *354*(2), 497–503.
Schuler, B., & Eaton, W. A. (2008). Protein folding studied by single-molecule FRET. *Current Opinion in Structural Biology*, *18*(1), 16–26.
Shank, E. A., Cecconi, C., Dill, J. W., Marqusee, S., & Bustamante, C. (2010). The folding cooperativity of a protein is controlled by its chain topology. *Nature*, *465*(7298), 637–640.
Shaw, D. E., Maragakis, P., Lindorff-Larsen, K., Piana, S., Dror, R. O., Eastwood, M. P., et al. (2010). Atomic-level characterization of the structural dynamics of proteins. *Science*, *330*(6002), 341–346.
Sirinakis, G., Ren, Y., Gao, Y., Xi, Z., & Zhang, Y. (2012). Combined versatile high-resolution optical tweezers and single-molecule fluorescence microscopy. *The Review of Scientific Instruments*, *83*(9), 093708.
Smith, S. B., Cui, Y., & Bustamante, C. (2003). Optical-trap force transducer that operates by direct measurement of light momentum. *Methods in Enzymology*, *361*, 134–162.
Stamp, M., & Le, E. (2005). Hamptonese and hidden Markov models. In W. Dayawansa, A. Lindquist, & Y. Zhou (Eds.), *New directions and applications in control theory*; *Vol. 321*, (pp. 367–378). Berlin, Heidelberg: Springer.
Steward, A., Toca-Herrera, J. L., & Clarke, J. (2002). Versatile cloning system for construction of multimeric proteins for use in atomic force microscopy. *Protein Science*, *11*(9), 2179–2183.
Stigler, J., & Rief, M. (2012). Calcium-dependent folding of single calmodulin molecules. *Proceedings of the National Academy of Sciences of the United States of America*, *109*, 17814–17819.
Stigler, J., Ziegler, F., Gieseke, A., Gebhardt, J. C., & Rief, M. (2011). The complex folding network of single calmodulin molecules. *Science*, *334*(6055), 512–516.
Tanford, C. (1970). Protein denaturation. C. Theoretical models for the mechanism of denaturation. *Advances in Protein Chemistry*, *24*, 1–95.
Teilum, K., Olsen, J. G., & Kragelund, B. B. (2011). Protein stability, flexibility and function. *Biochimica et Biophysica Acta*, *1814*(8), 969–976.
Thirumalai, D., Klimov, D. K., & Woodson, S. A. (1997). Kinetic partitioning mechanism as a unifying theme in the folding of biomolecules. *Theoretical Chemistry Accounts*, *96*(1), 14–22.
Tinoco, I., Jr., & Bustamante, C. (2002). The effect of force on thermodynamics and kinetics of single molecule reactions. *Biophysical Chemistry*, *101–102*, 513–533.
Tinoco, I., Jr., & Gonzalez, R. L., Jr. (2011). Biological mechanisms, one molecule at a time. *Genes & Development*, *25*(12), 1205–1231.
Tompa, P. (2011). Unstructural biology coming of age. *Current Opinion in Structural Biology*, *21*(3), 419–425.
Tskhovrebova, L., Trinick, J., Sleep, J. A., & Simmons, R. M. (1997). Elasticity and unfolding of single molecules of the giant muscle protein titin. *Nature*, *387*(6630), 308–312.
Wensley, B. G., Batey, S., Bone, F. A., Chan, Z. M., Tumelty, N. R., Steward, A., et al. (2010). Experimental evidence for a frustrated energy landscape in a three-helix-bundle protein family. *Nature*, *463*(7281), 685–688.
West, D. K., Olmsted, P. D., & Paci, E. (2006). Mechanical unfolding revisited through a simple but realistic model. *The Journal of Chemical Physics*, *124*(15), 154909.

Wright, C. F., Lindorff-Larsen, K., Randles, L. G., & Clarke, J. (2003). Parallel protein-unfolding pathways revealed and mapped. *Nature Structural Biology*, *10*(8), 658–662.

Xi, Z., Gao, Y., Sirinakis, G., Guo, H., & Zhang, Y. (2012). Single-molecule observation of helix staggering, sliding, and coiled coil misfolding. *Proceedings of the National Academy of Sciences of the United States of America*, *109*(15), 5711–5716.

Yang, G., Cecconi, C., Baase, W. A., Vetter, I. R., Breyer, W. A., Haack, J. A., et al. (2000). Solid-state synthesis and mechanical unfolding of polymers of T4 lysozyme. *Proceedings of the National Academy of Sciences of the United States of America*, *97*(1), 139–144.

Yu, H., Gupta, A. N., Liu, X., Neupane, K., Brigley, A. M., Sosova, I., et al. (2012). Energy landscape analysis of native folding of the prion protein yields the diffusion constant, transition path time, and rates. *Proceedings of the National Academy of Sciences of the United States of America*, *109*(36), 14452–14457.

Yu, H., Liu, X., Neupane, K., Gupta, A. N., Brigley, A. M., Solanki, A., et al. (2012). Direct observation of multiple misfolding pathways in a single prion protein molecule. *Proceedings of the National Academy of Sciences of the United States of America*, *109*, 5283–5288.

Zoldak, G., & Rief, M. (2013). Force as a single molecule probe of multidimensional protein energy landscapes. *Current Opinion in Structural Biology*, *23*(1), 48–57.

Zwanzig, R., Szabo, A., & Bagchi, B. (1992). Levinthal's paradox. *Proceedings of the National Academy of Sciences of the United States of America*, *89*(1), 20–22.